Journal of Inorganic Biochemistry 104 (2010) 774–789

Contents lists available at ScienceDirect

Journal of Inorganic Biochemistry

journal homepage: www.elsevier.com/locate/jinorgbio

Tautomerization of 2-nitroso-*N*-arylanilines by coordination as *N*,*N*′-chelate ligands to rhenium(I) complexes and the anticancer activity of newly synthesized oximine rhenium(I) complexes against human melanoma and leukemia cells *in vitro* ☆

Stefan Wirth [a], Andreas U. Wallek [a], Anna Zernickel [a], Florian Feil [a], M. Sztiller-Sikorska [b], K. Lesiak-Mieczkowska [b], Christoph Bräuchle [a], Ingo-Peter Lorenz [a,*], M. Czyz [b,*]

[a] Ludwig-Maximilians University Munich, Department of Chemistry and Biochemistry, Butenandtstr. 5-13 (House D), D-81377 Munich, Germany
[b] Medical University of Lodz, Department of Molecular Biology of Cancer, 6/8 Mazowiecka, 92-215 Lodz, Poland

ARTICLE INFO

Article history:
Received 6 November 2009
Received in revised form 24 March 2010
Accepted 26 March 2010
Available online 1 April 2010

Keywords:
Rhenium
Oximine
N,*N*′-chelates
In vitro anticancer activity
Melanoma
Leukemia

ABSTRACT

The synthesis, structural characterization and biological activity of eight *ortho*-quinone(*N*-aryl)-oximine rhenium(I) complexes are described. The reaction of the halogenido complexes $(CO)_5ReX$ (X=Cl (**4**), Br (**5**)) with 2-nitroso-*N*-arylanilines {$(C_6H_3ClNO)NH(C_6H_4R)$} (R=*p*-Cl, *p*-Me, *o*-Cl, H) (**3a**–**d**) in tetrahydrofurane (THF) yields the complexes *fac*-$(CO)_3XRe\{(C_6H_3ClNO)NH(C_6H_4R)\}$ (**6a**–**d**, **7a**–**d**) with the tautomerized ligand acting as a *N*,*N*′-chelate. The substitution of two carbonyl ligands leads to the formation of a nearly planar 5-membered metallacycle. During coordination the amino-proton is shifted to the oxygen of the nitroso group which can be observed in solution for **6** and **7** by ^1H NMR spectroscopy and in solid state by crystal structure analysis. After purification, all compounds have been fully characterized by their ^1H and ^{13}C NMR, IR, UV/visible (UV/Vis) and mass spectra. The X-ray structure analyses revealed a distorted octahedral coordination of the CO, X and *N*,*N*′-chelating ligands for all Re(I) complexes. Biological activity of four oximine rhenium(I) complexes was assessed *in vitro* in two highly aggressive cancer cell lines: human metastatic melanoma A375 and human chronic myelogenous leukemia K562. Chlorido complexes (**6a** and **6c**) were more efficient than bromido compounds (**7d** and **7b**) in inducing apoptotic cell death of both types of cancer cells. Melanoma cells were more susceptible to tested rhenium(I) complexes than leukemia cells. None of the ligands (**3a**–**d**) showed any significant anticancer activity.

1. Introduction

The chemistry of *C*-nitroso compounds started in 1874 with the synthesis of 4-nitroso-*N*,*N*′-dimethylaniline [1] and nitrosobenzene [2] by A. von Baeyer. Their first coordination to metals (Cd(II) and Zn(II)) was reported by Pickard and Kenyon in 1907 [3]. Since then a considerable variety of synthetic routes to high-yield preparations of *C*-nitroso compounds has been developed. The most up to date reviews on this topic have been recently published [4,5]. Not only due to its rich coordination chemistry [6] the family of *C*-nitroso compounds has been extensively investigated during the last decades. Its relevance in organic chemistry [7] was first proved 1899 by the Ehrlich–Sachs reaction [8]. Examples published in recent years are application in *ene* reactions [9] or hetero Diels–Alder reactions [10–12]. The discovery of the important roles of *C*-nitroso compounds in various biological metabolic processes [13–21] has also generated a renewed interest in this class of compounds.

In this context the convenient availability of 2-nitroso-*N*-arylanilines [22] has drawn our attention from *N*,*O*-bridging [23–25] and -chelating [26] to *N*,*N*′-chelating ligands. Before 2007 this class of compounds was mostly reported as a by-product [27–29]. Examples are the photochemical cyclization of *N*-acyl-2-nitroarylanilines [30,31] or the Fischer–Hepp rearrangement [32]. Only two comparable compounds with additional functional groups (methyl 6-hydroxy-4-methyl-3-nitroso-2-(phenylamino)benzoate [33] and 2-nitroso-1,3,5-*tris*(phenylamino)benzene [34]) were obtainable in good yields earlier. In coordination chemistry this ligand system is mentioned in few binuclear Pd(II) complexes [35–38]. There, it is formed by the reaction of a tetranuclear Pd(I) cluster with nitrosoarenes. Contrary to these results, the reaction of 2-nitroso-*N*-arylanilines with Re(I) halogenido complexes of the type $Re(CO)_5X$ (X=Cl, Br) leads to a metal-induced tautomerization. An *o*-quinoid system is formed and the amino-proton is shifted to the oxygen of the nitroso group. In this report we describe the synthesis and characterization of eight Re(I) complexes showing this tautomeric behaviour and the results of testing for biological activity of four of these complexes. We have

☆ Dedicated to Prof. Dr. Hubert Schmidbaur on the Occasion of his 75th Birthday.

* Corresponding authors. Fax: +49 89 2180 77867.
E-mail addresses: ipl@cup.uni-muenchen.de (I.-P. Lorenz), malgorzata.czyz@umed.lodz.pl (M. Czyz).

0162-0134/$ – see front matter © 2010 Elsevier Inc. All rights reserved.
doi:10.1016/j.jinorgbio.2010.03.014

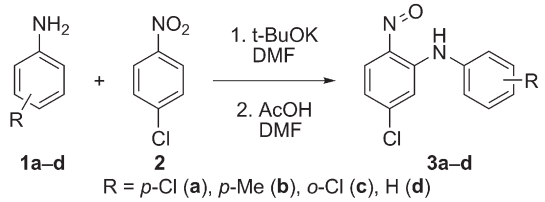

Scheme 1. Synthesis of *C*-nitroso compounds **3a–d**.

selected **6a**, **6c**, **7d**, and **7b** for biological studies. The cytotoxicity of the drugs was evaluated in A375, a human melanoma cell line exhibiting high metastatic potential, and K562, a Bcr–Abl-positive human chronic myelogenous leukemia (CML) cell line derived from a patient in blast crisis.

Metal-induced tautomerization reactions have been examined especially in relation with Pt(II) pyrimindine [39] and adenine [40] model nucleobase interactions. In these examples a shift of the equilibrium to the "wrong" tautomer could lead to base-mispairing in nucleic acids. Moreover, metal-induced proton migration in complexes is an important attribute in connection with the design of molecular electronic devices [41]. The capacity of intercalation into DNA [42,43] and in general the strong metal–ligand π-interaction have also attracted great interest into *o*-quinone ligand systems. Much literature on this topic is concerned with *o*-quinoid diimines [44–48], less with dioximes [49–52], but to the best of our knowledge the Re(I) complexes presented here are the first combining the imine and the oxime function in one and the same *o*-quinoid system.

2. Results and discussion

2.1. Synthesis and characterization of ligands 3a–d

The 2-nitroso-*N*-arylaniline ligands **3a–d** were synthesized in a one-pot reaction from anilines **1a–d** and 1-chloro-4-nitrobenzene (**2**) with potassium-*tert*-butoxide and acetic acid in dimethylformamide (DMF) (Scheme 1). Modifications made on this literature method [22] are described in the experimental section.

The synthesis yields ligands **3a–d** as air stable, dark green or brown powders, soluble for example in dichloromethane, tetrahydrofurane or acetone and nearly insoluble in pentane or *n*-hexane. Mass spectrometric investigation in the direct electron-impact ionization mode with detection of positive ions (DEI^+) shows the expected [M^+] peak and an assignable fragmentation pattern for all ligands. In the ^1H NMR of **3a–d** spectra a broad singlet in the range of 11.60 to 12.06 ppm can be identified as the amino-proton signal. Another broad singlet at $\delta = 8.64–8.66$ ppm can be assigned to the proton in *ortho*-position of the NO-group. The remaining signals of the protons in *meta*-position and the second aromatic ring are observed at $\delta = 6.93–7.52$ ppm. Exemplarily the ^{13}C NMR spectrum of **3c** is depicted in Fig. 1.

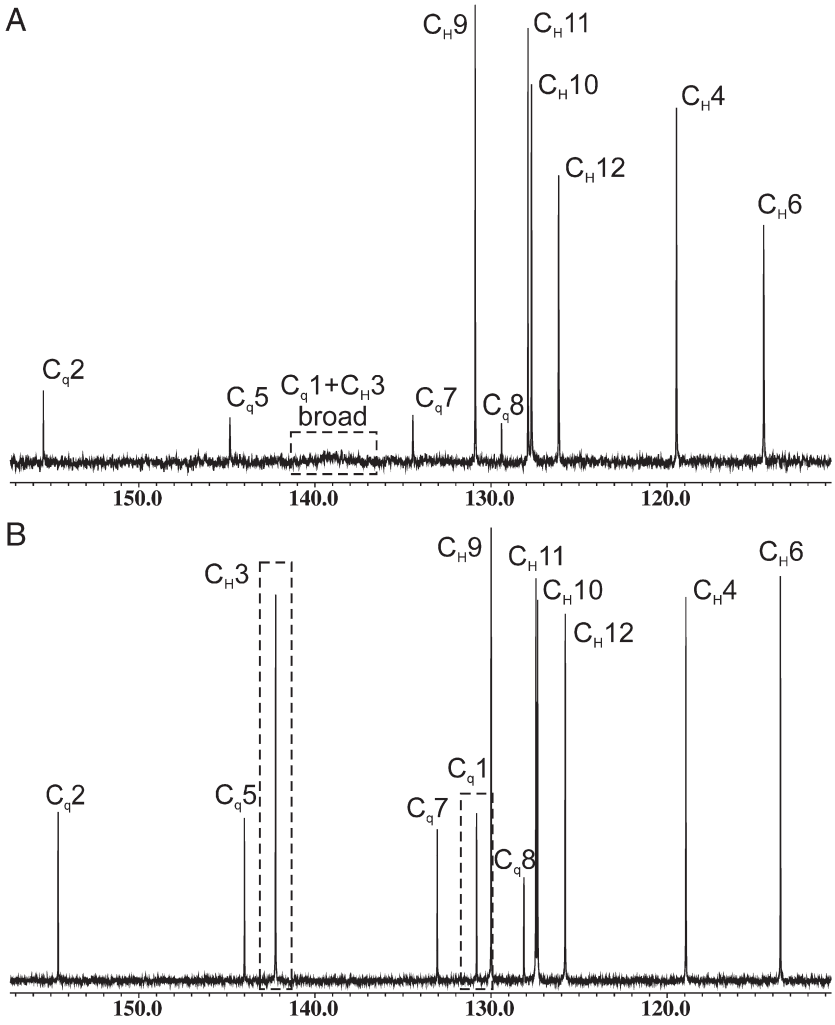

Fig. 1. ^{13}C NMR spectra of **3c** at A) 25 °C and B) −60 °C.

For each ligand one C_q and one C_H peak was "missing" and a very broad signal around 140 ppm could be detected at room temperature (Fig. 1). Measurement at −60 °C shows two "new" peaks at 130.8 (C_q1) and 142.2 ppm (C_H3) which can be assigned to the carbons in *ortho*-position of the nitroso group. "Freezing" rotation along the C–N bond leads to a significant splitting of the broad signal ($\Delta = 11.4$ ppm). This is induced of course by the different substituents but in fact more due to the large magnetic anisotropy [53] of the NO-group. This effect of an asymmetric substituent upon the relative chemical shifts of the *ortho*-carbons is a known phenomenon and established for aromatic nitroso compounds [54,55].

The IR spectra of ligand **3a–d** (KBr pellets) show ν(C–H) absorptions between 3100 and 2900 cm^{-1} but lack a pronounced ν(N–H) band, apparently as a consequence of the strong intramolecular hydrogen bonding [32]. Therefore, a broad and weak absorption between 2900–2650 cm^{-1} is observed due to N…H…O bonding. Surprisingly a very weak absorption for ν(N–H) is detected in liquid phase IR spectra at higher wave numbers (**3a**: 3372 cm^{-1}; **3b**: 3377 cm^{-1}; **3c**: 3373 cm^{-1}; **3d**: 3378 cm^{-1} in CH_2Cl_2). Nitroso stretching absorptions are assigned according to the reports of Gowenlock et al. in the range of 1488–1513 cm^{-1} for monomeric aromatic ArNO compounds [21,55,56]. The allocation of these bands is supported due to the fact that they disappear after complexation. This demonstrates the fundamental change in chemical character of the N—O bond when tautomerization from nitroso to oxime happens.

Measurement of UV/Vis spectra of **3a–d** in dichloromethane revealed four intense absorptions for each ligand (Table 1). Three are located in the UV area and are originated from π–π* transitions of the aromatic rings. The fourth is situated in the visible range and is identified as π–π* NO transition.

Since no crystallographic information was available for this compound class in the literature, molecular structures of **3b** (Fig. 2) and **3d** have been determined by X-ray diffraction analysis. Single crystals were obtained by slow sublimation at 55 °C and 1.0×10^{-3} mbar. The structure analysis revealed two planar aromatic rings (C(1)–C(6) and C(7)–C(12)) whereas the first ring shows some quinoid contribution. C—C bond lengths for C(3)—C(4) and C(5)–C(6) are noticeable shortened in comparison to the remaining aromatic ring. Furthermore

Table 1
UV/Vis absorption data of **3a–3d** and **6a–7d**: in CH_2Cl_2 λ_{max} [nm] (ε [M^{-1} cm^{-1}]) and fluorescence data of **3c** and **6a–7d** in CH_2Cl_2 λ_{max} [nm].

	UV	Visible
3a	253(13300), 278(17100), 312(14900)	461(8200)
3b	249(12900), 269(12100), 312(12700)	467(6900)
3c	253(12000), 275[a](15500), 312[a] (13400)	457(7200)
λ_{em}	523[b] 523[b]	
3d	250(12000), 274(12400), 312(12400)	464(6800)
6a	321(4500)	471(4500), 548[a](9700)
λ_{em}		607[b]
6b	320(4500)	474(5200), 541[a](10500)
λ_{em}		573[b]
6c	322[a](6400)	438(4500), 470(4800), 555[a] (12600)
λ_{em}	510[b]	606[b]
6d	321(4900)	470(4800), 544[a](11200)
λ_{em}		612[b]
7a	358(6200)	475(5400), 549[a](11000)
λ_{em}		600[c]
7b	357(5400)	481(5500), 544[a](9900)
λ_{em}		586[c]
7c	362(6400)	441(3800), 474(4400), 557[a] (11200)
λ_{em}		601[c]
7d	358(5600)	473(4700), 546[a](9800)
λ_{em}		608[c]

[a] Excitation at the marked absorption peak.
[b] Accuracy of the measurement: **3c**, **6a–d**: ±3 nm.
[c] Accuracy of the measurement: **7a–d**: ±10 nm.

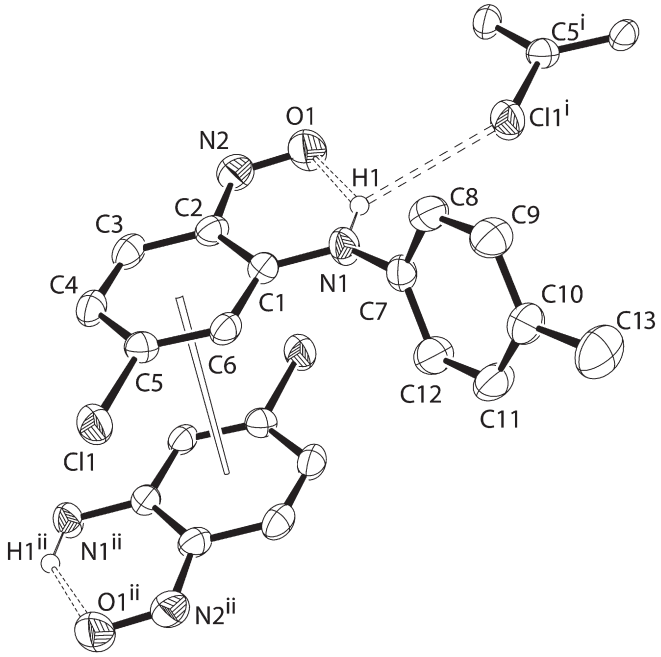

Fig. 2. Molecular structure of 5-Chloro-2-nitroso-N-p-tolylaniline (**3b**) with π–π stacking (open bond) and 3-centered intermolecular hydrogen bond (dashed lines). The thermal ellipsoids are drawn at the 50% probability level [57]. Aromatic and aliphatic hydrogen atoms as well as parts of further molecules of **3b** are omitted for clarity.

C—N bond lengths of N(1)–C(1) and N(2)–C(2) are always a bit shorter than N(1)–C(7). In both cases the nitroso group, located in the plane of the C(1)–C(6) ring and the amine, is stabilized by an intramolecular hydrogen bond. N—O bond lengths are in the expected range (1.13–1.29 Å) [21] for nitrosoarenes.

In both structures a secondary intermolecular interaction of the amine proton forms a 3-centered hydrogen bond. In **3b** the intermolecular acceptor is chlorine (Cl(1)) (Fig. 2). For **3d** the additional acceptor is a nitroso oxygen whereas the interacting molecule forms a second "back bonding" H-bridge. As further intermolecular interaction a π–π stacking [58,59] of the C(1)–C(6) ring occurs (Fig. 2). In the unit cell of **3b** for example, two of these rings show absolutely coplanar arrangement with a plane-to-plane distance of 3.50 Å. A parallel displacement of only 1.00 Å is calculated for the centroids. For **3d** a slight deviation from coplanarity is observed.

2.2. Synthesis and characterization of Re(I) complexes **6a–7d**

The novel oximine rhenium(I) complexes (**6a–7d**) are obtained as illustrated in Scheme 2. Refluxing $Re(CO)_5X$ (X=Cl (**4**), Br (**5**)) in dry THF leads to the substitution of two CO ligands. Completeness of the replacement can be monitored with liquid phase IR spectroscopy by a shift of the ν(CO) bands.

Addition of one equivalent of **3a–d** in dry THF and workup as described in the experimental section yields the complexes **6a–7d** quantitatively. Complexes **6a–7d** are obtained as dark green (**6a–7b**) or dark purple (**7c**, **7d**) powders. They are slowly decomposing when exposed to moist air, soluble in dichloromethane or chloroform and insoluble in pentane. Mass spectrometric investigations of complexes **6a–7d** (FAB^+ mode) exhibit the parent peak as well as a comparable fragmentation pattern resulting from successive loss of CO and halogenido ligands.

Comparison of the ^{1}H NMR spectra of **6a–7d** with the corresponding ligand spectra (**3a–d**) shows similar tendencies. In all

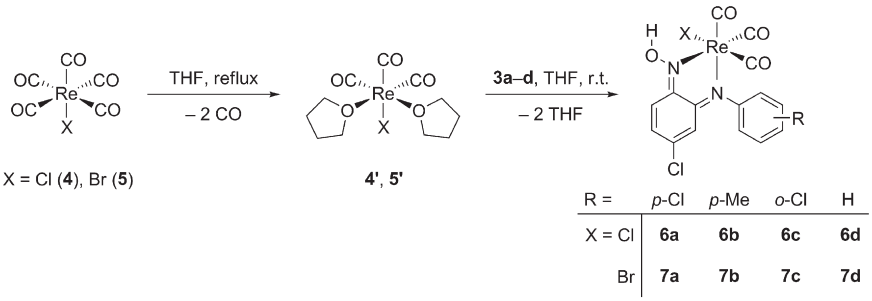

Scheme 2. Synthesis of the *N*,*N*′-chelate complexes **6a**–**7d**.

cases the broad singlet of the acidic proton shows a large shift to higher field due to migration from the amino group (**3a**–**d**: 11.60–12.06 ppm) to the nitroso oxygen (**6a**–**7d**: 8.31–9.50 ppm). All three signals of the *ortho*-quinoid system are shifted to higher field after coordination. The protons of the second, aromatic ring of complexes **6a**–**7d** show no consistent tendencies compared to the ligand spectra. In the ^{13}C NMR spectra of **6a**–**7d** all signals for the CO ligands, the quaternary aromatic carbons and the aromatic C_H carbons are detected in the expected areas. Since rotation of the nitroso group along C(2)–N(2) is inhibited after coordination, all signals are observable separately at room temperature. In comparison to the starting materials **3a**–**d** no general direction of the shifts can be identified in products **6a**–**7d**.

IR spectra of **6a**–**7d** in liquid phase show three intense ν(CO) absorptions. This is in accordance with C_S–symmetry of their *facial* arrangement. Surprisingly measurement of **7a**–**7d** in KBr pellets exhibit up to five ν(CO) bands what apparently can be caused by packing effects in solid state. In the area around 3000 cm^{-1} ν(C–H) absorptions are detected overlapping with a broad band between 3050 and 3200 cm^{-1} attributed to ν(O—H). Comparison of IR data of different transition metal complexes containing an oxime or oximine function [60–64] with spectra of **6a**–**7d** leads to the following assignment: absorptions at 1597–1606 cm^{-1} to ν(C=N) of the imine moiety, bands from 1543–1553 cm^{-1} to ν(C=N) of the oxime moiety. The interval associated with ν(N—O) (1040–1060 cm^{-1}) shows two strong absorptions very close together for each complex, again caused by packing effects.

The UV/Vis spectroscopic investigations of **6a**–**7d** in CH_2Cl_2 revealed typically three and in two cases (**6c** and **7c**) four absorptions. One is located in the UV area and is caused by a d^6-metal-to-ligand charge-transfer transition, the rest appears in the visible range. The difference of about 30 m between chlorido (**6a**–**6d**) and bromido complexes (**7a**–**7d**) may be caused by their different ligandfield strength. The stronger absorptions in the visible region arise from π–π* transitions of the ligand, mostly with no distinct maxima, shifted there by its tautomerization into an *o*-quinoid form. All spectra show this bathochromic shift in comparison to the corresponding electronic transitions of **3a**–**d** (Table 1). Compounds **6a**–**7d** showed weak fluorescence in the visible range with a fluorescence quantum yield of about 10^{-5}. Excitation at the absorption maxima of **6a**–**7d** at around 550 nm resulted in fluorescence maxima at around 610 nm (Table 1). For bromido complexes **7a**–**7d** the signal to noise ratio (SNR) was at the detection limit and about one order of magnitude lower than the SNR of **6a**–**6d** with chlorido ligand. Therefore the error of the fluorescence maxima position is significantly increased. That in consideration, the fluorescence maxima position of the chlorido complex compared with the corresponding bromido complex seems to be similar, while the different ligands (**3a**–**d**) have a small influence on the maxima. It is noteworthy that the ligand in its aromatic form (only tested for **3c**) exhibited also very weak fluorescence at around 523 nm when exciting at 275 nm or 312 nm, but not around 610 nm. This indicates that the fluorescence at 510 nm in **6c** is only caused by the rhenium carbonyl part and that around 610 nm results from the ligand which has been changed into its *o*-quinoid form showing lower frequencies. Selected fluorescence spectra are available as supporting information.

The molecular structures of complexes **6a**–**7d** were determined by X-ray diffraction analysis. Single crystals were obtained by isothermic diffusion of *n*-pentane into a solution of **6a**–**7d** in CH_2Cl_2 or $CHCl_3$. The X-ray structure analysis revealed a distorted octahedral coordination for all Re(I) complexes, consisting of the CO, halogenido and *N*,*N*′-chelating ligands **3a**–**d**.

Crystal data and details of structure refinement for compounds **3b**, **3d** and **6a**–**7d** are summarized in Table 5. Selected bond lengths and angles are listed in Table 2. Exemplarily, only **6a** is depicted in Fig. 3, ORTEP-plots of all other structures and hydrogen bond data are

Table 2
Selected bond lengths (Å) and angles (°) of compounds **3b**, **3d** and **6a**–**7d**.

Compound	3b	3d	6a	6b	6c	6d	7a	7b	7c	7d
Re(1)–C(13)/C(14) **6b**	–	–	1.948(4)	1.943(4)	1.947(7)	1.904(12)	1.951(4)	1.936(5)	1.962(8)	1.927(7)
Re(1)–C(14)/C(15) **6b**	–	–	1.921(4)	1.937(3)	1.937(7)	1.927(10)	1.937(4)	1.936(5)	1.912(8)	1.932(7)
Re(1)–C(15)/C(16) **6b**	–	–	1.911(4)	1.897(4)	1.913(8)	1.904(12)	1.905(5)	1.899(6)	1.913(10)	1.901(8)
Re(1)–Cl **6**/Br **7**	–	–	2.481(1)	2.486(1)	2.480(2)	2.478(2)	2.621(1)	2.623(1)	2.614(1)	2.636(1)
Re(1)–N(1)	–	–	2.120(3)	2.134(3)	2.129(5)	2.134(7)	2.133(3)	2.133(3)	2.128(6)	2.129(4)
Re(1)–N(2)	–	–	2.141(3)	2.139(3)	2.136(5)	2.136(7)	2.120(3)	2.127(3)	2.137(5)	2.112(5)
O(1)–N(2)	1.258(2)	1.259(2)	1.384(3)	1.374(3)	1.369(7)	1.379(8)	1.370(3)	1.375(4)	1.379(7)	1.309(6)
N(2)–C(2)	1.388(2)	1.382(2)	1.298(4)	1.312(4)	1.308(8)	1.304(11)	1.310(4)	1.312(5)	1.303(8)	1.345(7)
C(1)–C(2)	1.434(3)	1.430(2)	1.460(5)	1.461(4)	1.456(9)	1.468(12)	1.456(5)	1.456(6)	1.471(9)	1.447(7)
N(1)–C(1)	1.350(2)	1.357(2)	1.310(4)	1.314(4)	1.313(8)	1.333(10)	1.315(4)	1.319(5)	1.314(9)	1.314(7)
N(1)–C(7)	1.431(2)	1.420(2)	1.451(4)	1.439(4)	1.439(8)	1.441(11)	1.433(4)	1.437(5)	1.448(9)	1.431(7)
N(1)–Re(1)–N(2)	–	–	73.27(10)	73.90(9)	73.8(2)	73.8(3)	73.95(11)	73.71(13)	73.7(2)	74.99(17)
C(13)/C(14) **6b**–Re(1)–N(2)	–	–	104.13(13)	103.04(11)	103.1(2)	103.1(3)	99.88(13)	100.67(16)	103.5(2)	96.4(2)
C(14)/C(15) **6b**–Re(1)–N(1)	–	–	94.83(13)	95.15(11)	95.1(2)	96.5(3)	96.57(14)	97.54(16)	95.4(3)	96.5(2)
N(2)–Re(1)–N(1)–C(1)	–	–	4.3(2)	8.9(2)	1.8(5)	−7.1(6)	−4.7(2)	5.1(3)	1.4(5)	1.4(4)
C(1)–N(1)–C(7)–C(12)	74.4(3)	62.2(3)	69.8(4)	76.1(4)	96.4(8)	−110.2(10)	−103.9(4)	117.7(5)	99.7(8)	69.1(7)

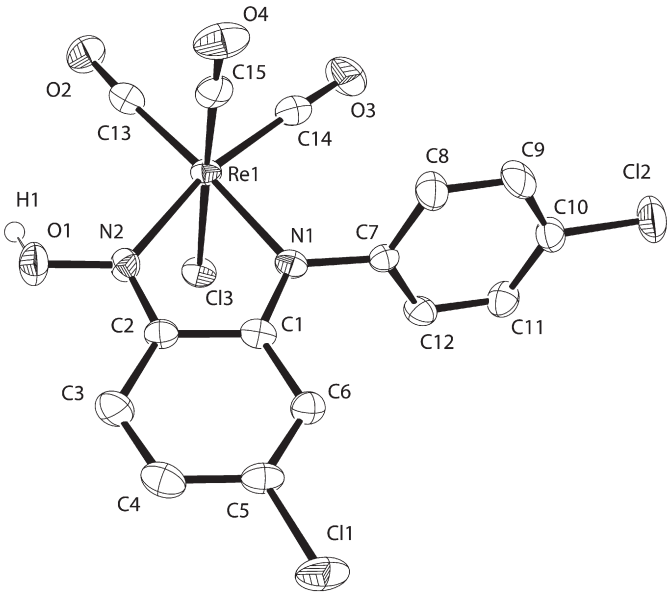

Fig. 3. Molecular structure of Tricarbonyl-chlorido-{4-chloro-*o*-quinone-(*N*-4-chlorophenyl)-oximine-*N,N′*}rhenium(I) (**6a**). The thermal ellipsoids are drawn at the 50% probability level [57]. Aromatic hydrogen atoms are omitted for clarity.

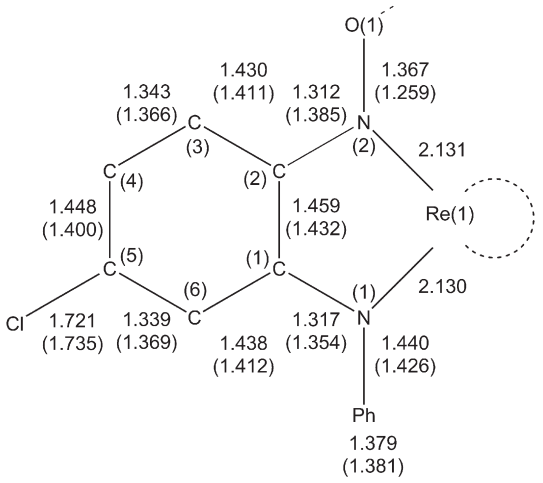

Scheme 3. Average bond lengths of **6a**–**7d** in comparison with average values in **3b** and **3d** (in brackets).

available as supporting information. Bond lengths Re–CO are in the expected range for *fac*-Re(CO)$_3$X-complexes with quinoid ligands [46,65], just as well as the Re–X (X=Cl, Br) bonds. The Re—CO$_{ax}$ bond in *trans*-position to the halogenido ligand is considerably shorter than the Re—CO$_{eq}$ bonds. This indicates a π-accepting character of the *N,N′*-chelates. Re–N distances in **6a**–**7d** show no recognizable preference for a shorter imine or oxime bonding and are close to bond lengths recently reported for an *ortho*-quinoid diimine Re(I) complex [46] or a Re(I) nitroso complex [66]. Only few structurally characterized rhenium oximato complexes suitable for comparison are known. Re–N bond lengths observed in **6a**–**7d** are slightly longer than reported for an oximato ligand chelating Re(V) (2.099(3) Å) [67] or a dioxime ligand system chelating Re(III) (2.028(9)–2.108(9) [68] / 2.03(1)–2.17(1) [69]). Crystallographic information for Re(I) is only available for a monodentating, nonaromatic oximato ligand. This shows a somewhat longer Re—N bond length (2.183(6) Å) [70] than **6a**–**7d**.

After coordination the former aromatic system of **3a**–**d** with only some quinoid contribution shows clearly quinoid topology. A significant elongation of the N—O bond (Scheme 3) to an expected scale (1.319(4) Å [67], 1.368 Å [69], 1.396(9) Å [70]) confirms the oxime nature of the former nitroso group. Shortening of N(1)–(C1) and N(2)–C(2) and explicitly alternating C—C bond lengths indicate the *o*-quinoid form of the C(1)–C(6) ring. This is also in accordance to a recently published bond length pattern for *o*-quinoid ligands in different oxidation states[71]. The effect of coordination to rhenium on the average bond lengths in the second aromatic ring is negligible.

The bidentate ligands **3a**–**d** bind to rhenium(I) via formation of a nearly planar metallacycle. This is confirmed by torsion angels close to 0° within the 5-membered ring. Distortion of the octahedral coordination sphere becomes evident by the small ligand bite angles N(1)–Re–N(2) around 74° and the angles between the chelating nitrogen atoms and the equatorial carbonyls. Complexes **6a**–**7d** exhibit on the oxime-side (N(2)–Re(1)–CO$_{eq}$) an average angle of 101.7°. The imine-side (N(1)–Re(1)–CO$_{eq}$) shows values close to 95°. The bridging nitrogen atom (N1) is trigonal planar in geometry consistent with its sp^2 nature, whereas the sum of surrounding angles is always very close to 360°.

The second aromatic ring connected to N(1) is highly turned out of the plane defined by the metallacycle (69.1(7)°–117.7(5)°). A dependence of this angle on the ligands was not identifiable. This may be an effect of π–π-interaction between the aromatic or quinoid rings since in every structure an absolute coplanar arrangement of these moieties is observed. An exception is given in **7d** where only some rings of the same type are coplanar. For complexes **6a**–**7c** a triclinic crystal system in the space group *P*-1 is observed, containing two complex molecules in the unit cell. An intermolecular hydrogen bond connects the oxime function of one molecule and the halogenido ligand of another molecule in the next unit cell and vice versa. Thus each of these pairs is connected through two intermolecular hydrogen bonds. In complex **7d** a monoclinic crystal system in the space group *C*2/*c* with eight molecules in one unit cell is observed. The only difference to **6a**–**7c** is the lack of intermolecular hydrogen bonds between complex molecules of **7d**. Instead of these, a hydrogen bond to the CH_2Cl_2 enclosed in the cell is observed. This may be the reason for the discrepancy. Apparently intermolecular hydrogen bonds between the complex molecules are an integral factor in the arrangement within the unit cell of these compounds.

2.3. Biological evaluation

2.3.1. Oximine rhenium(I) complexes inhibit melanoma adherent cell proliferation more efficiently than proliferation of leukemia cells

Concentration–response and time course analyses were performed using four rhenium(I) complexes (**6a**, **6c**, **7d**, and **7b**). In some experiments, the 2-nitroso-*N*-arylaniline ligands (**3a**–**3d**) were included. Tetrazolium derivative reduction (MTT) assay was used to assess the influence of the drugs on the metabolic activity of adherent melanoma cells (A375) in relation to untreated control cells. Cell proliferation of leukemic K562 cells cultured in suspension was determined using Trypan blue dye exclusion assay. First, IC$_{50}$ values were estimated for the cancer cell inhibition of proliferation as shown in Fig. 4. IC$_{50}$ values obtained for melanoma A375 cells treated with **6a**, **6c**, **7d**, and **7b** for 2 days were 0.9, 0.7, 1.3, and 1.8 μM, respectively (Fig. 4A).

Higher concentrations of oximine rhenium(I) complexes were necessary to reduce proliferation of K562 cells to 50% compared to the control cells (Fig. 4B). But similarly to the results obtained for melanoma cells, **6a** and **6c** were more efficient in induction of growth arrest (IC$_{50}$ of 3.4 and 3 μM, respectively) than **7d** and **7b** with IC$_{50}$ of 7.5 μM and 7.8 μM, respectively. Ligand **3c** reduced cell proliferation to 96% and 90% compared to the control cells when it was used at the concentrations of 4 μM and 8 μM, respectively. The other ligands were also much less efficient than their respective rhenium(I) complexes (not shown).

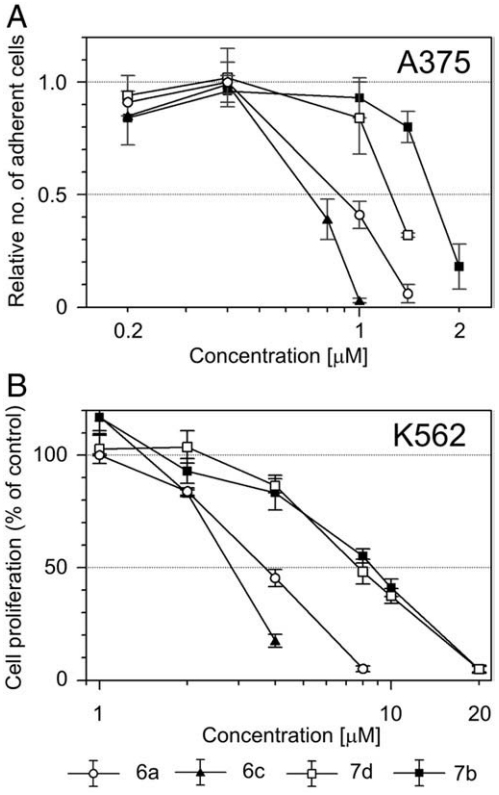

Fig. 4. Concentration–response analyses of the influence of oximine rhenium(I) complexes on melanoma and leukemia cell proliferation. (A) MTT assay was used to study cytostatic effects of oximine rhenium(I) complexes in human melanoma cell line A375. The mean of the absolute absorbance values given by drug-treated cells was divided by the mean of the absolute absorbance of DMSO-treated control sample and expressed as relative number of viable adherent cells. (B) Trypan blue exclusion test was applied to assess cytostatic effects of the tested drugs in human CML cell line K562 as described in Materials and Methods. Cell proliferation is expressed as the percentage of viable cell number in the control culture. IC50 values for each compound in each cell line were calculated (see text for the results). The data are the mean ± SD of three independent experiments done in triplicates.

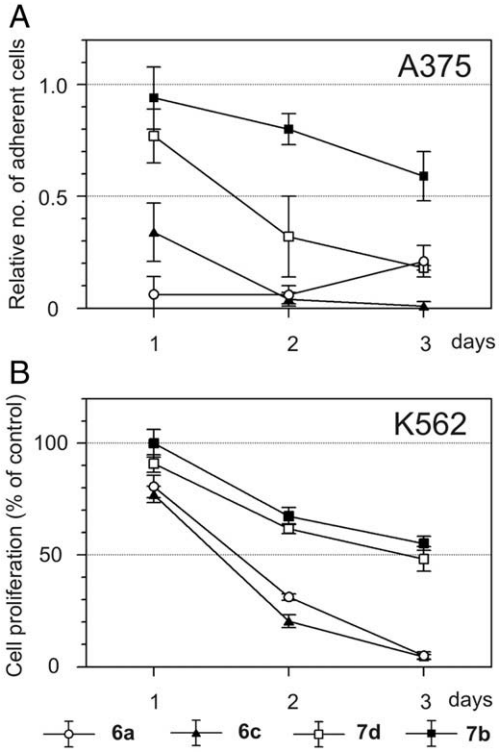

Fig. 5. Oximine rhenium(I) complexes inhibit melanoma (A) and leukemia (B) cell proliferation. A time course. A375 cells were treated with 1.4 μM and K562 cells with 8 μM oximine rhenium(I) complexes for up to 3 days. Viable, adherent A375 melanoma cells were quantified daily by MTT assay and viable K562 leukemia cells by Trypan blue exclusion test. The data are the mean ± SD of three independent experiments done in triplicates ($P<0.05$ except for **7b** on day 1).

Next, time course analyses were performed. Viable melanoma cells were quantified daily by MTT assay, leukemia cells were evaluated by Trypan blue staining (Fig. 5).To get similar reduction of proliferation in both cell lines, concentrations of drugs used in these experiments were 1.4 μM in A375 cell cultures (Fig. 5A) and 8 μM in K562 cell cultures (Fig. 5B). As expected **6c** and **6a** were more efficient than **7d** and **7b** in both cell types.

2.3.2. Effects of oximine rhenium(I) complexes on cancer cell viability

Changes in A375 melanoma cell viability in response to oximine rhenium(I) complexes were assessed by propidium iodide staining and FACS analysis (Fig. 6). On the second day of treatment, only **6c** at the concentration of 1 μM significantly reduced the viability of melanoma cells to 53% (47% ± 5 of cells were PI-positive; $P<0.05$). The other oximine rhenium(I) complexes (**6a**, **7b**, and **7d**) applied at the concentration of 1 μM or ligands (**3a**–**d**) used at the concentration of 2 μM did not induce the appearance of PI-permeable cells. When concentration of rhenium(I) complexes was raised to 2 μM viability of melanoma cells was decreased to the level below 30%.

Trypan blue exclusion test was used to assess viability of K562 cells treated with oximine rhenium(I) complexes. In this assay, the number of dead cells taking up Trypan blue was expressed as percentage of the total cell number (viable and dead) in each experimental condition. First, K562 cells were treated continuously for 3 days with 8 μM of the oximine rhenium(I) complexes. On day 3, similar effectiveness was observed for **6c** and **6a**, whereas **7d** and **7b** were still ineffective (Fig. 7A). When the viability of K562 cells was tested at the concentrations of drugs in the range from 1 μM to 100 μM, **6c** and **6a** reduced viability to 50% of the control at the concentrations of 7 μM and 8 μM, respectively. The same was observed for **7d** and **7b** at concentrations as high as 33 μM and 29 μM, respectively (Fig. 7B). Ligands **3a**–**d** did not significantly affect K562 cell viability even at the concentration of 20 μM (not shown).

2.3.3. Induction of apoptosis in A375 melanoma cells and K562 leukemic cells by oximine rhenium(I) complexes

Cell death was assessed in melanoma cells treated with oximine rhenium(I) complexes by morphological characteristics of apoptotic and necrotic cells in fluorescence microscopy after staining with acridine orange and ethidium bromide (AO/EB) (Fig. 8). More than 300 cells were analyzed and then the percentages of early/late apoptotic or necrotic cells were calculated. Compound **6c**, which most efficiently reduced proliferation of adherent melanoma cells, induced apoptosis in more than 80% of the cells when applied at the concentrations of 1 μM and 2 μM (Table 3). For **6a** and **7d**, concentration of 2 μM was required to stimulate apoptosis to this extent. Compound **7b**, the least efficient in inhibiting proliferation of adherent melanoma cells, was also the least effective in inducing cell death. None of the tested drugs, including ligands, stimulated necrosis in melanoma cells. Therefore, we could assume that in the applied conditions apoptotic cell death was the major cause of reduced proliferation of melanoma cells.

Bcr–Abl-expressing leukemic K562 cells are highly resistant to apoptosis induced by chemotherapeutic agents. In the current study, they were assessed on day 3 for the evidence of apoptotic cell death by double staining with AO/EB (Fig. 9A). In addition, DAPI staining was used to show the condensation and fragmentation of the nuclei (Fig. 9B). Neither DAPI staining nor double staining with AO/EB for early and late apoptosis showed an induction of apoptosis after 3 days

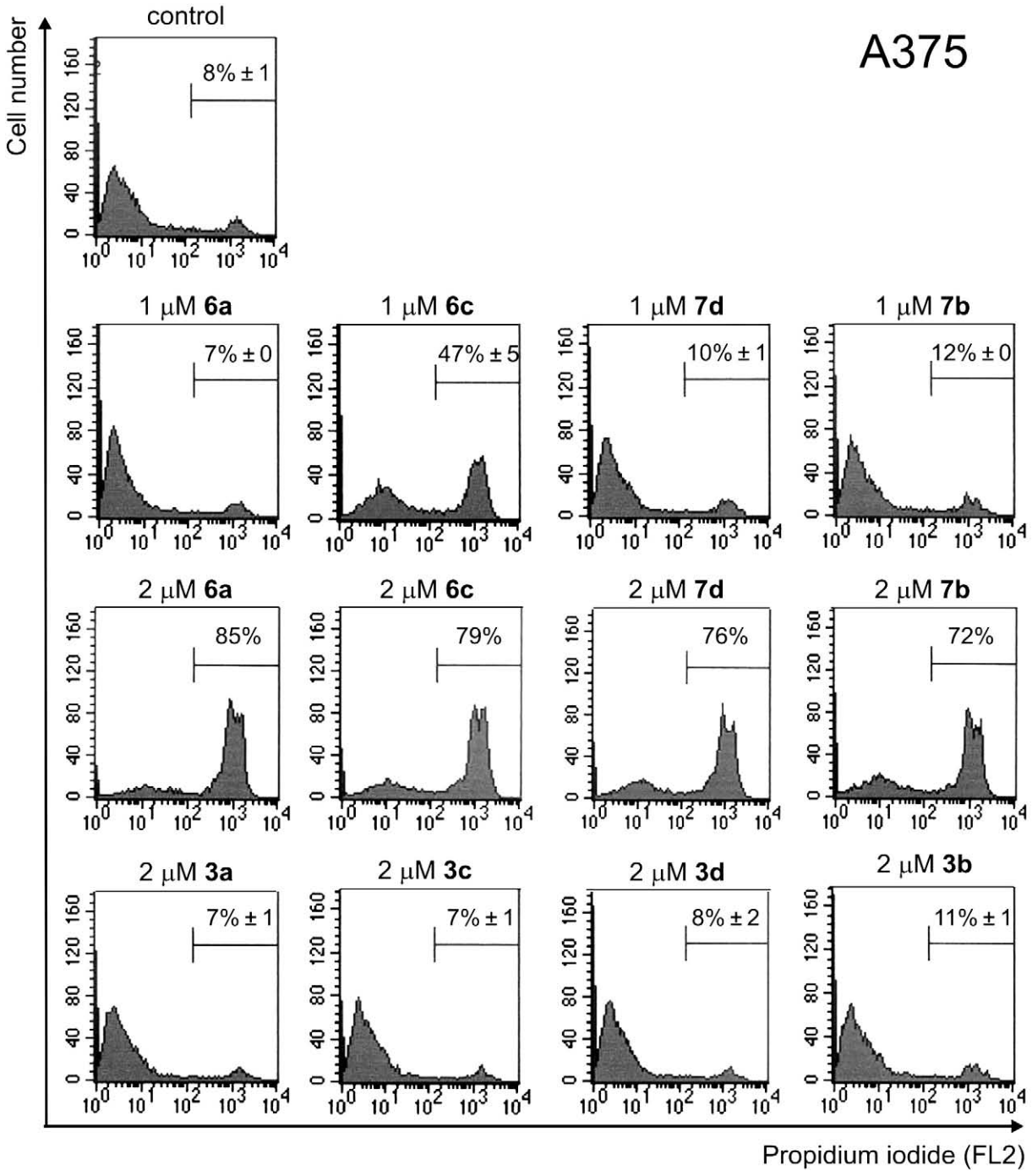

Fig. 6. Effects of the oximine rhenium(I) complexes on melanoma cell viability. A375 melanoma cells were treated for 2 days with **6c**, **6a**, **7d**, and **7b** at concentrations of 1 μM and 2 μM, or with ligands **3a**–**d** at the concentration of 2 μM. The percentages of cells with PI-permeable membrane were assessed by FACS analysis in combined populations of adherent and floating cells. Selected histograms from a representative experiment are shown. The data are the mean ± SD of two independent experiments ($P<0.05$) except from 2 μM oximine rhenium(I) complexes when only one experiment was done.

of treatment with 8 μM **7d** and **7b**. At the same concentration, **6c** and **6a** induced apoptotic cell death in the majority of K562 cells. More than 90% of cells were either in early or late stage of apoptosis after 3 days of treatment with these drugs (Table 4). Compound **6c** was the most efficient in induction of apoptosis. This was clearly visible in the experiment showing fragmented nuclei which appeared in the presence of **6c** at a concentration as low as 4 μM (Fig. 9B). As expected, ligands (**3a**–**d**) did not induce apoptotic cell death when used at concentrations of 8 μM and 20 μM. Necrosis was also not induced in these conditions.

In summary, current studies of anticancer activity of four oximine rhenium(I) complexes performed in melanoma and leukemia cell lines have revealed that in two series of halogenido Re(I) complexes (X=Cl, Br), chlorido complexes were more efficient as anticancer drugs *in vitro*. Chlorido complexes **6c** and **6a** possessed significant cytostatic activity against leukemia K562 cells and melanoma A375 cells. This activity was much higher than for bromido compounds **7d** and **7b**. Lethal effects of chlorido Re(I) complexes in melanoma and leukemia cells were obtained at different concentrations of compounds. Chlorido Re(I) complexes at the concentration of 1 μM were

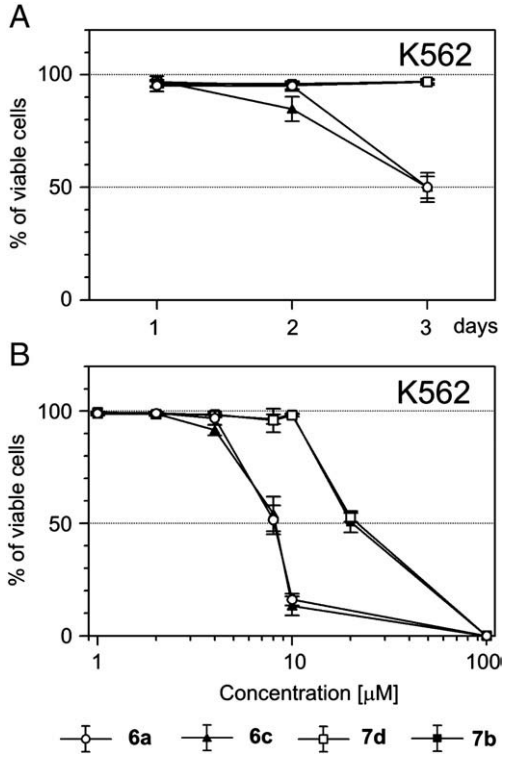

Fig. 7. Effects of the oximine rhenium(I) complexes on leukemia cell viability. (**A**) Aliquots of K562 cell cultures treated with 8 μM oximine rhenium(I) complexes **6c**, **6a**, **7d**, and **7b** were removed daily for a determination of the number of viable and dead cells by Trypan blue exclusion test. The number of viable cells is expressed as percentage of total cell number. (**B**) K562 cells were treated with oximine rhenium(I) complexes at different concentrations and the number of viable and dead cells was assessed on day 3 by Trypan blue exclusion test. The data are the mean ± SD of two independent experiments done in triplicates ($P<0.05$).

apparently effective in stimulating cell death only in melanoma cells, **6c** was the most efficient in this respect. In leukemic K562 cells, higher concentrations were necessary to achieve a similar level of inhibition, but again compound **6c** was the most effective. Comparison of cytotoxic and cytostatic effects revealed that apoptotic cell death, defined as loss of cell membrane integrity, was the major cause of reduced proliferation in melanoma and leukemia cells. This was assessed in A375 melanoma cells as PI- and AO/EB-membrane permeability and in K562 leukemia cells as Trypan blue- and AO/EB-membrane permeability, and shown as nuclei fragmentation. Bromido compounds **7d** and **7b** were much less effective against melanoma and leukemia cells, however, **7d** exerted some effect on proliferation of adherent melanoma cells. It is also interesting that among chlorido and bromido complexes, those having ligand with no substituent in *para* position (**6c** and **7d**) showed higher cytotoxic activity than those with either methyl (**7b**) or chlorine (**6a**) substituents. It is of note that ligands themselves (**3a**–**d**) did not stimulate cellular death in melanoma and leukemia cells. The relationship between chemical structure and the vulnerability of cancer cells to drug-induced apoptosis needs to be further explored.

K562 cell line derived from a patient in blast crisis is commonly accepted as a cellular model of advanced phase of chronic myelogenous leukemia (CML) [72,73]. It was reported by many groups that commonly used anticancer drugs do not efficiently induce apoptosis in K562 cells, mainly due to the constitutive Bcr–Abl activity and a negligible level of p53. Only imatinib, by directly targeting activity of fusion kinase Bcr–Abl, induces mitochondria-dependent apoptosis in K562 cell line [73]. Therefore, the results obtained for the newly synthesized oximine rhenium(I) complexes suggested that at least a part of the cytotoxic activity of these compounds might be connected with Bcr–Abl pathway.

Melanoma is the most aggressive type of skin cancer and is highly resistant to all currently used chemotherapeutics [74]. The alkylating drug dacarbazine (DTIC), which is approved for treatment of metastatic melanoma, results in clinical responses of 5–10% of patients [75]. Human A375 melanoma cell line used in our study, is considered as having high metastatic potential and is highly resistant to anticancer drugs. Therefore, the obtained results with oximine rhenium(I) complexes, especially those chlorido compounds **6c** and **6a**, are encouraging and need further investigation. One reason for higher susceptibility of melanoma cells than leukemia cells to Re(I) complexes could be the influence of the drugs on the adhesive potential of melanoma cells. In addition to clearly visible apoptosis induced by oximine rhenium(I) complexes, they might affect cell adhesion. By reducing the number of adherent cells in culture they could influence the relative number of cells able to proliferate. It should also be taken into account, that any single-agent chemotherapy tested in clinical setting for melanoma patients has resulted in response rates below 20%.[76,77] Therefore, instead of oximine rhenium(I) complexes alone, combination with other drugs, including those highly specific for deregulated pathways in melanoma cells, should be considered for future evaluations.

Taken together, our data demonstrated that albeit to different extent, newly synthesized oximine rhenium(I) complexes investigated in this study could induce apoptotic cell death in leukemia and melanoma cells. To our knowledge, this is the first study showing the anticancer therapeutic potential of rhenium complexes against melanoma and leukemia cells. Further studies are necessary to unravel the exact mechanism(s) of the cellular responses evoked by these compounds as well to verify their effectiveness in *in vivo* models.

3. Experimental

3.1. General

All experiments and manipulations were performed under dry argon atmosphere using Schlenk and vacuum-line techniques. $Re(CO)_5X$ (X=Cl (**4**), Br (**5**)) [78] were prepared according to a literature procedure. The published synthesis of 2-nitroso-*N*-arylanilines [22] (**3a**–**d**) has to be modified to achieve good yields. Solvents were purified by standard procedures; dichloromethane was distilled from calcium hydride, *n*-pentane and *n*-heptane were distilled from lithium aluminium hydride and tetrahydrofurane was distilled from sodium. All solvents were stored under a dry argon atmosphere with 3 Å molecular sieves (dichloromethane) respectively sodium pieces (*n*-pentane, *n*-heptane, THF). NMR spectra were recorded with a Jeol Eclipse 270, Jeol Eclipse 400 or Jeol EX 400 spectrometer at ambient temperature unless stated otherwise. All chemical shifts are given in ppm relative to TMS. The splitting of proton resonances in the reported ^{1}H NMR spectra is defined as s = singlet, d = doublet, dd = doublet of doublets, ddd = doublet of doublets of doublets, dddd = doublet of doublets of doublets of doublets, m = multiplet and br s = broad singlet. IR spectra were measured in the range of 4000–400 cm^{-1} using a PerkinElmer Spectrum One FT-IR spectrometer. The intensity of reported IR signals is defined as vs = very strong, s = strong, m = medium and w = weak. UV/visible (UV/Vis) data was recorded with a Varian Cary 50 UV/Vis spectrophotometer. The emission spectra were recorded on a FS900 fluorescence spectrometer (Edinburgh Analytical Instruments). Mass spectra were obtained by a Jeol MStation JMS-700 in direct electron-impact ionization mode (DEI) or positive ion fast atom bombardment ionization mode (FAB^+) (3-nitrobenzyl alcohol (NBA) matrix). Multi-isotope containing fragments refer to the isotope with the highest abundance. Elemental analyses were performed with

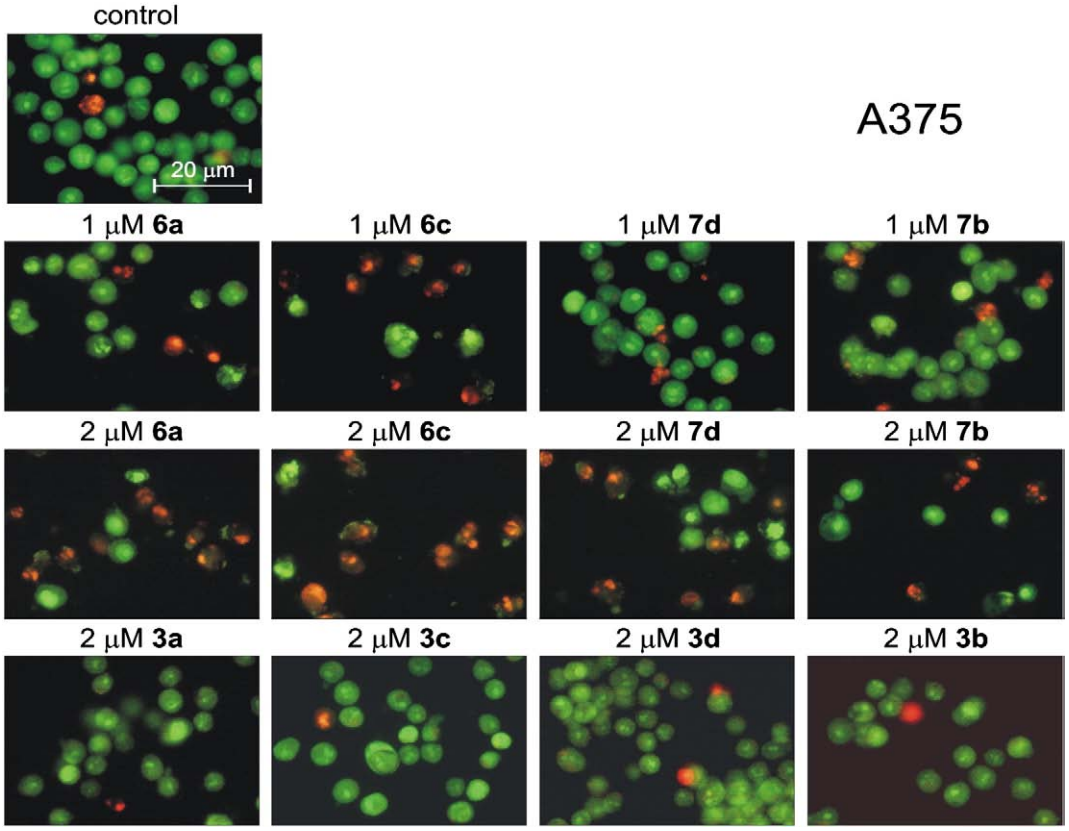

Fig. 8. The oximine rhenium(I) complexes induce apoptosis but not necrosis in melanoma cells. Double staining of A375 melanoma cells following 2 day exposure to oximine rhenium(I) complexes at the concentrations of 1 μM and 2 μM. Cells were stained with nucleic acid selective fluorochromes: membrane-permeable acridine orange and impermeable ethidium bromide. Representative microscopic fields are shown. Viable cells had bright green chromatin with organized structure. In early apoptotic cells, the chromatin was condensed or fragmented but still stained green. In late apoptotic cells, it was condensed or fragmented and stained orange. Necrotic cells had bright orange chromatin with organized structure. Ten different fields were randomly selected for counting 300 cells and the percentages of early and late apoptotic cells, and necrotic cells were calculated. Quantitative data are presented in Table 3.

a Heraeus elementar varioEL by the Micoanalytical Laboratory of the Department of Chemistry and Biochemistry, LMU.

3.2. Synthesis of ligands **3a–d**

A solution of *t*BuOK (24 mmol, 2.69 g) in 8 mL DMF was cooled (acetone/dry ice/−78 °C) till it was nearly freezing. First a cooled solution of aniline **1a–d** (8 mmol) in 4 mL DMF (change of colour to light yellow or green), then a cooled solution of 1-chloro-4-nitrobenzene (**2**) (8 mmol) in 4 mL DMF was added dropwise (change of colour to purple). After stirring at this temperature for 5–10 min a cooled mixture of conc. AcOH (6 mL) in DMF (6 mL) was added (change of colour to brown). The solution was allowed to reach room temperature, poured into water and extracted three times with EtOAc. The combined organic layers were washed three times with water, one time with brine, then a solution of $NaHCO_3$ and water again, then dried with Na_2SO_4. After evaporation the crude product was purified by column chromatography on silica gel (dichloromethane–pentane).

Table 3
Dual staining with acridine orange and ethidium bromide indicates an induction of apoptosis but not necrosis after 2 days of treatment of melanoma A375 cells with indicated concentrations of tested compounds.

	[μM]	Early apoptosis	Late apoptosis	Necrosis
Control	–	1	6	2
6a	1	11	**23**	1
	2	**17**	**73**	1
6c	1	**29**	**50**	1
	2	**14**	**70**	9
7d	1	3	10	1
	2	**26**	**54**	4
7b	1	3	11	1
	2	**15**	**43**	3
3c	2	2	2	5

A minimum of 300 cells was counted and all four cellular states were recorded. Then, the percentages of early or late apoptotic or necrotic cells were calculated. Bold data points indicate significant differences ($P<0.05$) from the control data points.

3.2.1. 5-Chloro-N-(4-chlorophenyl)-2-nitrosoaniline (**3a**)

Reagents: 1.02 g (8.00 mmol) **1a**, 1.26 g (8.00 mmol) **2**. Yield: 1.01 g (3.78 mmol, 47%), brown powder. — ^{1}H NMR (400 MHz, $CDCl_3$): $\delta = 6.99$ (dd, $^3J_{H,H} = 8.7$ Hz, $^4J_{H,H} = 1.7$ Hz, 1 H, H4), 7.05 (d, $^4J_{H,H} = 1.9$ Hz, 1 H, H6), 7.18–7.23 (m, 2H, H8 + H12), 7.39–7.44 (m, 2H, H9 + H11), 8.65 (br s, 1H, H3), 11.81 (br s, 1H, NH) ppm. ^{13}C NMR (100 MHz, $CDCl_3$): $\delta = 114.3$ (C6), 119.3 (C4), 126.3 (C8 + C12), 130.2 (C9 + C11), 132.5 (C10), 135.2 (C7), 141.2 (br, C1 + C3), 145.0 (C5), 155.2 (C2) ppm. IR (KBr, cm^{-1}): $\tilde{\nu} = 2963$ (w), 2925 (w), 2854 (w), 1612 (m), 1592 (s), 1560 (s), 1504 ν(N=O) (m), 1489 (m), 1462 (m), 1338 (m), 1262 (s), 1154 (vs), 1106 (vs), 1092 (vs), 1012 (m), 942 (m), 809 (s), 798 (vs), 560 (m). UV/Vis (CH_2Cl_2): λ_{max} (ε) = 253 (13,300), 278 (17,100), 312 (14,900), 461 nm (8200 M^{-1} cm^{-1}). MS (DEI): *m/z* (%) = 266.2 (13) [M^+], 249.2 (100) [M^+–H–O], 235.2 (29) [M^+–H–NO], 231.2 (16) [M^+–Cl], 214.2 (4) [M^+–Cl–OH], 201.2 (28) [M^+–Cl–NO], 166.2 (16) [M^+–2Cl–NO]. $C_{12}H_8Cl_2N_2O$ (267.11 g mol^{-1}): calcd. C 53.96, H 3.02, N 10.49; found C 53.88, H 3.13, N 10.38.

3.2.2. 5-Chloro-2-nitroso-N-p-tolylaniline (**3b**)

Reagents: 857 mg (8.00 mmol) **1b**, 1.26 g (8.00 mmol) **2**. Yield: 873 mg (3.54 mmol, 44%), dark green powder. Green crystals were

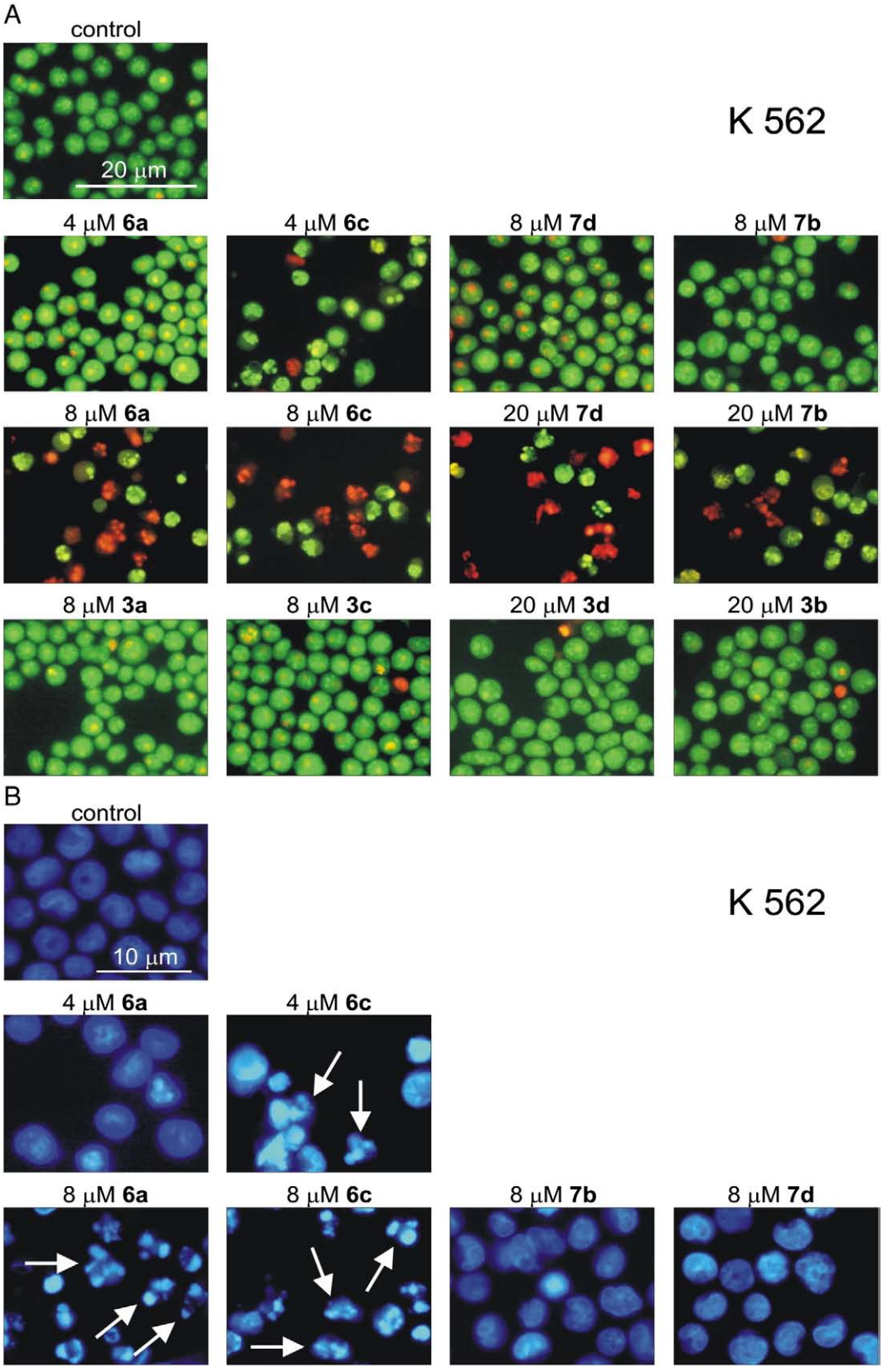

Fig. 9. The oximine rhenium(I) complexes induce apoptosis but not necrosis in leukemia cells. (A) Double staining of K562 leukemia cells following 3 day exposure to oximine rhenium(I) complexes at the indicated concentrations. The microscopic fields obtained for K562 cells exposed to ligands **3a**–**c** are included. Quantitative data are presented in Table 4. (B) K562 cells were stained with DAPI for nuclear fragmentation and analyzed by fluorescence microscopy. Arrows indicate some examples of cells with fragmented nuclei.

obtained by slow sublimation of **3b** at 55 °C and 1.0×10^{-3} mbar. – ^{1}H NMR (270 MHz, $CDCl_3$): $\delta = 2.39$ (s, 3H, CH_3), 6.93 (dd, $^{3}J_{H,H} = 8.8$ Hz, $^{4}J_{H,H} = 1.9$ Hz, 1H, H4), 7.05 (d, $^{4}J_{H,H} = 2.0$ Hz, 1H, H6), 7.10–7.16 (m, 2H, H8 + H12), 7.21–7.27 (m, 2H, H9 + H11), 8.65 (br s, 1H, H3), 12.06 (br s, 1H, NH) ppm. ^{13}C NMR (100 MHz, $CDCl_3$): $\delta = 21.2$ (CH_3), 114.6 (C6), 118.7 (C4), 125.1 (C8 + C12), 130.6 (C9 + C11), 133.7 (C7),

Table 4
Dual staining with acridine orange and ethidium bromide indicates an induction of apoptosis but not necrosis after 3 days of treatment of K562 cells with indicated concentrations of tested drugs.

	[μM]	Early apoptosis	Late apoptosis	Necrosis
Control	–	0.2	0.8	1.3
DMSO	–	0.3	0.7	1.0
6a	4	2.4	1.8	1.0
	8	**45.0**	**51.6**	0.5
6c	2	0.0	1.5	1.2
	4	**30.1**	**12.9**	1.2
	8	**42.5**	**49.5**	1.0
7d	4	0.2	0.7	0.7
	8	2.4	2.5	0.5
	20	**51.2**	**45.1**	0.9
7b	8	0.2	2.2	0.7
	10	3.0	0.9	1.1
	20	**58.3**	**39.1**	0.2
3a	4	0.2	0.2	1.7
	8	0.6	0.9	1.6
3c	4	0.0	1.1	1.4
	8	0.2	0.9	2.1
3d	4	0.2	0.2	1.6
	8	0.1	0.8	1.0
	20	0.1	1.3	2.0
3b	4	0.0	0.3	0.9
	8	0.1	0.9	1.5
	20	0.0	1.7	2.3

A minimum of 300 cells was counted and all four cellular states were recorded. Then, the percentages of early or late apoptotic or necrotic cells were calculated. Bold data points indicate significant differences ($P<0.05$) from the control data points.

137.1 (C10), 141.7 (br, C1 + C3), 144.8 (C5), 155.2 (C2) ppm. IR (KBr, cm^{-1}): $\tilde{\nu}$ = 3084 (w), 3034 (w), 2913 (w), 1605 (m), 1554 (s), 1509 ν(N=O) (s), 1488 (s), 1436 (m), 1350 (m), 1333 (s), 1143 (s), 1100 (vs), 1175 (s), 1018 (m), 945 (m), 938 (m), 813 (m), 800 (s), 509 (m). UV/Vis (CH_2Cl_2): λ_{max} (ε) = 249 (12900), 269 (12100), 312 (12700), 467 nm (6900 M^{-1} cm^{-1}). MS (DEI): *m/z* (%) = 245.3 (6) [M^+–H], 229.3 (100) [M^+–H–O], 214.3 (19) [M^+–H–NO], 180.3 (17) [M^+–H–NO–Cl], 166.3 (5) [M^+–H–NO–Cl–Me]. $C_{13}H_{11}ClN_2O$ (246.69 g mol^{-1}): calcd. C 63.29, H 4.49, N 11.36; found C 63.39, H 4.27, N 11.32.

*3.2.3. 5-Chloro-N-(2-chlorophenyl)-2-nitrosoaniline (**3c**)*

Reagents: 1.02 g (8.00 mmol) **1c**, 1.26 g (8.00 mmol) **2**. Yield: 812 mg (3.04 mmol, 38%), brown powder. – ^{1}H NMR (270 MHz, $CDCl_3$): δ = 7.02 (dd, $^3J_{H,H}$ = 9.2 Hz, $^4J_{H,H}$ = 2.0 Hz, 1 H, H4), 7.02 (d, $^4J_{H,H}$ = 1.9 Hz, 1 H, H6), 7.24 (ddd, $^3J_{H,H}$ = 7.9 Hz, $^3J_{H,H}$ = 7.4 Hz, $^4J_{H,H}$ = 1.7 Hz, 1H, H10), 7.34 (ddd, $^3J_{H,H}$ = 7.9 Hz, $^3J_{H,H}$ = 7.4 Hz, $^4J_{H,H}$ = 1.6 Hz, 1H, H11), 7.46 (ddd, $^3J_{H,H}$ = 8.0 Hz, $^4J_{H,H}$ = 1.7 Hz, $^5J_{H,H}$ = 0.3 Hz, 1H, H12), 7.52 (ddd, $^3J_{H,H}$ = 7.9 Hz, $^4J_{H,H}$ = 1.6 Hz, $^5J_{H,H}$ = 0.4 Hz, 1 H, H9), 8.64 (br s, 1H, H3), 11.60 (br s, 1H, NH) ppm. ^{1}H NMR (400 MHz, $CDCl_3$, −60 °C): δ = 7.02 (d, $^4J_{H,H}$ = 1.8 Hz, 1H, H6), 7.06 (dd, $^3J_{H,H}$ = 8.7 Hz, $^4J_{H,H}$ = 1.8 Hz, 1H, H4), 7.25 (dd, $^3J_{H,H}$ = 7.6 Hz,$^3J_{H,H}$ = 7.6 Hz, 1H, H10), 7.34 (dd, $^3J_{H,H}$ = 7.6 Hz, $^3J_{H,H}$ = 7.6 Hz, 1H, H11), 7.45 (d, $^3J_{H,H}$ = 7.8 Hz, 1H, H12), 7.51 (d, $^3J_{H,H}$ = 7.9 Hz, 1H, H9), 8.88 (d, $^3J_{H,H}$ = 8.7 Hz, 1H, H3), 12.03 (br s, 1H, NH) ppm. ^{13}C NMR (68 MHz, $CDCl_3$): δ = 114.5 (C6), 119.5 (C4), 126.2 (C12), 127.7 (C10), 127.9 (C11), 129.4 (C8), 130.9 (C9), 134.4 (C7), 138.9 (br, C1 + C3), 144.8 (C5), 155.4 (C2) ppm. ^{13}C NMR (100 MHz, CD_2Cl_2, −60 °C): δ = 113.6 (C6), 118.9 (C4), 125.8 (C12), 127.4 (C10), 127.5 (C11), 128.1 (C8), 130.0 (C9), 130.8 (C1), 133.1 (C7), 142.2 (C3), 144.0 (C5), 154.6 (C2) ppm. IR (KBr, cm^{-1}): $\tilde{\nu}$ = 3086 (w), 2963 (w), 2923 (w), 1605 (s), 1589 (s), 1581 (s), 1565 (vs), 1506 ν(N=O) (m), 1476 (m), 1349 (m), 1339 (m), 1158 (s), 1105 (vs), 1079 (s), 946 (s), 804 (m), 750 (vs), 549 (m). UV/Vis (CH_2Cl_2): λ_{max} (ε) = 253 (12000), 275 (15500), 312 (13400), 457 nm (7200 M^{-1} cm^{-1}). MS (DEI): *m/z* (%) = 266.1 (6) [M^+], 249.1 (26) [M^+–H–O], 235.1 (14) [M^+–H–NO], 231.2 (100) [M^+−Cl], 216.2 (10) [M^+–Cl–O], 201.2 (13) [M^+–Cl–NO], 166.2 (14) [M^+–2Cl–NO]. $C_{12}H_8Cl_2N_2O$ (267.11 g mol^{-1}): calcd. C 53.96, H 3.02, N 10.49; found C 53.93, H 2.90, N 10.36.

*3.2.4. 5-Chloro-2-nitroso-N-phenylaniline (**3d**)*

Reagents: 745 mg (8.00 mmol) **1d**, 1.26 g (8.00 mmol) **2**. Yield: 775 mg (3.33 mmol, 42%), dark green powder. Green crystals were obtained by slow sublimation of **3d** at 55 °C and 1.0×10^{-3} mbar. – ^{1}H NMR (270 MHz, $CDCl_3$): δ = 6.96 (dd, $^3J_{H,H}$ = 8.8 Hz, $^4J_{H,H}$ = 2.0 Hz, 1H, H4), 7.11 (d, $^4J_{H,H}$ = 2.0 Hz, 1H, H6), 7.23–7.28 (m, 2H, H8 + H12), 7.28–7.34 (m, 1H, H10), 7.40–7.49 (m, 2H, H9 + H11), 8.66 (br s, 1H, H3), 12.02 (br s, 1H, NH) ppm. ^{13}C NMR (100 MHz, $CDCl_3$): δ = 114.5 (C6), 119.0 (C4), 125.1 (C8 + C12), 127.0 (C10), 130.0 (C9 + C11), 136.5 (C7), 141.4 (br, C1 + C3), 144.9 (C5), 155.2 (C2) ppm. IR (KBr, cm^{-1}): $\tilde{\nu}$ = 3084 (w), 3021 (w), 2924 (w), 1608 (m), 1587 (s), 1559 (vs), 1498 ν(N=O) (s), 1457 (m), 1354 (m), 1333 (m), 1160 (m), 1153 (m), 1098 (vs), 1081 (m), 1073 (m), 941 (m), 796 (m), 534 (s). UV/Vis (CH_2Cl_2): λ_{max} (ε) = 250 (12000), 274 (12400), 312 (12400), 464 nm (6800 M^{-1} cm^{-1}). MS (DEI): *m/z* (%) = 231.3 (9) [M^+–H], 215.3 (100) [M^+–H–O], 201.3 (25) [M^+–H–NO], 167.3 (23) [M^+–H–NO–Cl]. $C_{12}H_9ClN_2O$ (232.67 g mol^{-1}): calcd. C 61.95, H 3.90, N 12.04; found C 62.06, H 3.88, N 11.82.

3.3. Synthesis of complexes **6a–d** and **7a–d**

$Re(CO)_5X$ (X=Cl, Br) (**4** and **5**) was dissolved in 20 mL dry THF and refluxed for 20 h. The elimination of two CO ligands leading to the intermediates **4′** and **5′** could be observed by liquid phase IR spectroscopy in THF. The resulting pale-yellow mixture was added to a solution of one equivalent of ligand **3a–d** in 10 mL dry THF. Stirring at room temperature resulted in a change of colour from red brown to dark violet. Full conversion to the desired complexes **6a–d** and **7a–d** was again monitored by liquid phase IR spectroscopy after stated reaction time. After evaporation of nearly all THF (rest 2–3 mL) 30–40 mL of dry *n*-heptane was added and subsequently the solvent was again removed till complexes **6a–d** and **7a–d** precipitate as dark green or purple solids. After filtration the solids were washed four times with 5 mL dry *n*-heptane and dried in vacuo.

*3.3.1. Tricarbonyl-chlorido-{4-chloro-o-quinone-(N-4-chlorophenyl)-oximine-N,N′}rhenium(I) (**6a**)*

Reagents: 135 mg (0.373 mmol) **4**, 100 mg (0.373 mmol) **3a**, reaction time: 20 h. Yield: 196 mg (0.342 mmol, 92%), dark green powder. Dark red crystals were obtained by slow isothermic diffusion of *n*-pentane into a solution of **6a** in dichloromethane. – ^{1}H NMR (270 MHz, $CDCl_3$): δ = 6.70 (dd, $^4J_{H,H}$ = 1.8 Hz, $^5J_{H,H}$ = 0.7 Hz, 1H, H6), 6.86 (dd, $^3J_{H,H}$ = 10.0 Hz, $^4J_{H,H}$ = 1.8 Hz, 1H, H4), 6.99–7.10 (m, 1H, H8 or 12), 7.32–7.42 (m, 1H, H8 or 12), 7.52 (dd, $^3J_{H,H}$ = 9.9 Hz, $^5J_{H,H}$ = 0.7 Hz, 1H, H3), 7.52 (dd, $^3J_{H,H}$ = 7.6 Hz, $^4J_{H,H}$ = 1.5 Hz, 2H, H9 + H11), 9.43 (br s, 1H, NOH) ppm. ^{13}C NMR (100 MHz, $CDCl_3$): δ = 117.4 (C6), 118.2 (C3), 123.6 (C8 or 12), 124.7 (C8 or 12), 130.1 (C9 or 11), 130.4 (C9 or 11), 131.1 (C4), 134.4 (C10), 143.6 (C5), 147.8 (C7), 155.3 (C2), 163.7 (C1), 176.8 (CO), 193.7 (CO), 194.5 (CO) ppm. IR (KBr, cm^{-1}): $\tilde{\nu}$ = 3098 (w), 3084 (w), 2033 ν(CO) (vs), 1950 ν(CO) (vs), 1930 ν(CO) (vs), 1604 ν(C=N) (w), 1553 ν(C=N) (w), 1483 (m), 1421 (m), 1398 (w), 1303 (m), 1189 (m), 1161 (w), 1093 (w), 1054 ν(N–O) (m), 1045 ν(N–O) (m), 1013 (w), 931 (w), 829 (w), 803 (w), 586 (w) 543 (w), 518 (w), 444 (w). IR (THF, cm^{-1}): $\tilde{\nu}$ = 2029 ν(CO) (vs), 1952 ν(CO) (m), 1918 ν(CO) (m). **IR** (CH_2Cl_2, cm^{-1}): $\tilde{\nu}$ = 2033 ν(CO) (vs), 1954 ν(CO) m), 1926 ν(CO) (m). **UV/Vis** (CH_2Cl_2): λ_{max} (ε) = 321 (4500), 471 (4500), 548 nm (9700 M^{-1} cm^{-1}). MS (FAB$^+$): *m/z* (%) = 572.0 (76) [M^+], 544.1 (50) [M^+–CO], 537.1 (100) [M^+–Cl], 488.1 (78) [M^+–3CO], 453.1 (78) [M^+–3CO–Cl]. $C_{15}H_8Cl_3N_2O_4Re$ (572.80 g mol^{-1}): calcd. C 31.45, H 1.41, N 4.89; found C 31.28, H 1.39, N 4.72.

*3.3.2. Tricarbonyl-chlorido-{4-chloro-o-quinone-(N-p-tolyl)-oximine-N,N′}rhenium(I) (**6b**)*

Reagents: 133 mg (0.368 mmol) **4**, 91 mg (0.368 mmol) **3b**, reaction time: 22 h. Yield: 170 mg (0.308 mmol, 84%), dark green powder. Black crystals were obtained by slow isothermic diffusion of *n*-pentane into a solution of **6b** in chloroform. – ^{1}H NMR (270 MHz, $CDCl_3$): δ = 2.45 (s, 3 H, CH_3), 6.75 (dd, $^4J_{H,H}$ = 1.8 Hz, $^5J_{H,H}$ = 0.7 Hz, 1H, H6), 6.84 (dd, $^3J_{H,H}$ = 9.9 Hz, $^4J_{H,H}$ = 1.8 Hz, 1H, H4), 6.93–7.05 (m, 1H, H8 or 12), 7.29–7.35 (m, 3H, H9 + H11 + H8 or 12), 7.49 (dd, $^3J_{H,H}$ = 9.9 Hz, $^5J_{H,H}$ = 0.7 Hz, 1H, H3), 9.09 (br s, 1H, NOH) ppm. ^{13}C NMR (100 MHz, $CDCl_3$): δ = 21.4 (CH_3), 117.9 (C3), 118.0 (C6), 122.0 (C8 or 12), 123.2 (C8 or 12), 130.3 (C9 or 11), 130.6 (C9 or 11), 131.3 (C4), 138.8 (C10), 142.7 (C5), 147.1 (C7), 155.3 (C2), 163.2 (C1), 177.2 (CO), 193.9 (CO), 195.0 (CO) ppm. IR (KBr, cm^{-1}): $\tilde{\nu}$ = 3049 (w), 3025 (w), 2927 (w), 2032 ν(CO) (vs), 1955 ν(CO) (vs), 1937 ν(CO) (vs), 1605 ν(C=N) (m), 1599 (m), 1548 ν(C=N) (m), 1501 (m), 1421 (m), 1397 (m), 1296 (s), 1189 (m), 1161 (m), 1054 ν(N–O) (s), 1048 ν(N–O) (s), 1017 (w), 931 (w), 803 (m), 588 (w), 543 (w), 456 (w). IR (THF, cm^{-1}): $\tilde{\nu}$ = 2028 ν(CO) (vs), 1950 ν(CO) (m), 1916 ν(CO) (m). IR (CH_2Cl_2, cm^{-1}): $\tilde{\nu}$ = 2031 ν(CO) (vs), 1951 ν(CO) (s), 1924 ν(CO) (m). UV/Vis (CH_2Cl_2): λ_{max} (ε) = 320 (4500), 474 (5200), 541 nm (10500 M^{-1} cm^{-1}). MS (FAB^+): *m/z* (%) = 552.1 (71) [M^+], 524.1 (49) [M^+–CO], 517.1 (100) [M^+–Cl], 568.1.0 (84) [M^+–3CO], 433.1 (78) [M^+–Cl–3CO]. $C_{16}H_{11}Cl_2N_2O_4Re$ (552.38 g mol^{-1}): calcd. C 34.79, H 2.01, N 5.07; found C 35.05, H 2.12, N 5.15.

*3.3.3. Tricarbonyl-chlorido-{4-chloro-o-quinone-(N-2-chlorophenyl)-oximine-N,N′}rhenium(I) (**6c**)*

Reagents: 136 mg (0.376 mmol) **4**, 100 mg (0.376 mmol) **3c**, reaction time: 28 h. Yield: 194 mg (0.339 mmol, 90%), dark green powder. Brown crystals were obtained by slow isothermic diffusion of *n*-pentane into a solution of **6c** in dichloromethane. – ^{1}H NMR (400 MHz, CD_2Cl_2): δ = 6.57 (dd, $^4J_{H,H}$ = 1.8 Hz, $^5J_{H,H}$ = 0.7 Hz, 1H, H6), 6.91 (dd, $^3J_{H,H}$ = 10.0 Hz, $^4J_{H,H}$ = 1.9 Hz, 1H, H4), 7.39 (ddd, $^3J_{H,H}$ = 8.0 Hz, $^3J_{H,H}$ = 7.3 Hz, $^4J_{H,H}$ = 1.9 Hz, 1H, H10), 7.48 (ddd, $^3J_{H,H}$ = 7.9 Hz, $^3J_{H,H}$ = 7.2 Hz, $^4J_{H,H}$ = 1.4 Hz, 1H, H11), 7.53 (ddd, $^3J_{H,H}$ = 7.9 Hz, $^4J_{H,H}$ = 1.9 Hz, $^5J_{H,H}$ = 0.4 Hz, 1H, H12), 7.54 (dd, $^3J_{H,H}$ = 9.9 Hz, $^5J_{H,H}$ = 0.7 Hz, 1 H, H3), 7.60 (ddd, $^3J_{H,H}$ = 8.1 Hz, $^4J_{H,H}$ = 1.4 Hz, $^5J_{H,H}$ = 0.4 Hz, 1H, H9), 9.05 (br s, 1H, NOH) ppm. ^{13}C NMR (100 MHz, CD_2Cl_2): δ = 117.6 (C6), 117.7 (C3), 125.2 (C12), 126.1 (C8), 128.3 (C11), 129.4 (C10), 130.5 (C9), 131.1 (C4), 143.9 (C5), 146.0 (C7), 154.7 (C2), 164.5 (C1), 177.2 (CO), 194.2 (CO), 195.1 (CO) ppm. IR (KBr, cm^{-1}): $\tilde{\nu}$ = 3110 (w), 3070 (w), 2031 ν(CO) (vs), 1960 ν(CO) (vs), 1936 ν(CO) (vs), 1605 ν(C=N) (m), 1548 ν(C=N) (w), 1469 (m), 1421 (m), 1401 (w), 1297 (m), 1191 (w), 1161 (w), 1055 ν(N—O) (m), 1046 ν(N—O) (m), 935 (w), 800 (w), 763 (w), 740 (w) 623 (w), 588 (w), 547 (w), 456 (w). IR (THF, cm^{-1}): $\tilde{\nu}$ = 2029 ν(CO) (vs), 1953 ν(CO) (m), 1924 ν(CO) (m). IR (CH_2Cl_2, cm^{-1}): $\tilde{\nu}$ = 2033 ν(CO) (vs), 1953 ν(CO) (m), 1932 ν(CO) (m). UV/Vis (CH_2Cl_2): λ_{max} (ε) = 322 (6400), 438 (4500), 470 (4800), 555 nm (12600 M^{-1} cm^{-1}). MS (FAB^+): *m/z* (%) = 571.9 (75) [M^+], 544.0 (32) [M^+–CO], 537.1 (100) [M^+–Cl], 509.1 (13) [M^+–Cl–CO], 488.0 (26) [M^+–3CO], 481.1 (10) [M^+–Cl–2CO], 453.1 (54) [M^+–Cl–3CO], 452.1 (54) [M^+–Cl–3CO–H], 416.1 (18) [M^+–2Cl–3CO–H]. $C_{15}H_8Cl_3N_2O_4Re$ (572.80 g mol^{-1}): calcd. C 31.45, H 1.41, N 4.89; found C 31.52, H 1.51, N 4.81.

*3.3.4. Tricarbonyl-chlorido-{4-chloro-o-quinone-(N-phenyl)-oximine-N,N′}rhenium(I) (**6d**)*

Reagents Reagents: 147 mg (0.406 mmol) **4**, 94 mg (0.406 mmol) **3d**, reaction time: 22 h. Yield: 192 mg (0.357 mmol, 88%), dark green powder. Red crystals were obtained by slow isothermic diffusion of *n*-pentane into a solution of **6d** in dichloromethane. – ^{1}H NMR (400 MHz, CD_2Cl_2): δ = 6.75 (dd, $^4J_{H,H}$ = 1.7 Hz, $^5J_{H,H}$ = 0.5 Hz, 1H, H6), 6.89 (dd, $^3J_{H,H}$ = 10.0 Hz, $^4J_{H,H}$ = 1.8 Hz, 1H, H4), 7.10–7.16 (m, 1H, H8 or 12), 7.34–7.40 (m, 1H, H8 or 12), 7.43 (dddd, $^3J_{H,H}$ = 7.5 Hz, $^3J_{H,H}$ = 7.5 Hz, $^4J_{H,H}$ = 1.2 Hz, $^4J_{H,H}$ = 1.2 Hz, 1H, H10), 7.50 (dd, $^3J_{H,H}$ = 10.0 Hz, $^5J_{H,H}$ = 0.5 Hz, 1H, H3), 7.56 (ddd, $^3J_{H,H}$ = 7.5 Hz, $^3J_{H,H}$ = 7.5 Hz, $^4J_{H,H}$ = 1.3 Hz, 2H, H9 + H11), 8.94 (br s, 1H, NOH) ppm. ^{13}C NMR (100 MHz, CD_2Cl_2): δ = 117.8 (C3), 117.9 (C6), 122.2 (C8 or 12), 123.1 (C8 or 12), 128.4 (C10), 129.8 (C9), 129.8 (C11), 131.1 (C4), 143.1 (C5), 149.5 (C7), 155.5 (C2), 163.4 (C1), 177.6 (CO), 194.6 (CO), 195.6 (CO) ppm. IR (KBr, cm^{-1}): $\tilde{\nu}$ = 3054 (w), 3032 (w), 2935 (w), 2032 ν(CO) (vs), 1950 ν(CO) (vs), 1938 ν(CO) (vs), 1606 ν(C=N) (m), 1590 (w), 1548 ν(C=N) (w), 1451 (w), 1421 (m), 1398 (w), 1294 (s), 1187 (m), 1056 ν(N–O) (s), 1047 ν(N–O) (s), 940 (w), 856 (w), 802 (m), 703 (m), 626 (w), 587 (w) 544 (w). IR (THF, cm^{-1}): $\tilde{\nu}$ = 2029 ν(CO) (vs), 1951 ν(CO) (m), 1917 ν(CO) (m). IR (CH_2Cl_2, cm^{-1}): $\tilde{\nu}$ = 2032 ν(CO) (vs), 1952 ν(CO) (s), 1925 ν(CO) (s). UV/Vis (CH_2Cl_2): λ_{max} (ε) = 321 (4900), 470 (4800), 544 nm (11200 M^{-1} cm^{-1}). MS (FAB^+): *m/z* (%) = 538.0 (72) [M^+], 510.0 (45) [M^+–CO], 503.0 (100) [M^+–Cl], 454.0 (72) [M^+–3CO], 419.0 (68) [M^+–Cl–3CO]. $C_{15}H_9Cl_2N_2O_4Re$ (538.36 g mol^{-1}): calcd. C 33.46, H 1.69, N 5.20; found C 33.69, H 1.76, N 5.02.

*3.3.5. Bromido-tricarbonyl-{4-chloro-o-quinone-(N-4-chlorophenyl)-oximine-N,N′}rhenium(I) (**7a**)*

Reagents: 128 mg (0.315 mmol) **5**, 84 mg (0.315 mmol) **3a**, reaction time: 22 h. Yield: 169 mg (0.274 mmol, 87%), dark green powder. Brown crystals were obtained by slow isothermic diffusion of *n*-pentane into a solution of **7a** in dichloromethane. – ^{1}H NMR (400 MHz, $CDCl_3$): δ = 6.74 (dd, $^4J_{H,H}$ = 1.8 Hz, $^5J_{H,H}$ = 0.7 Hz, 1H, H6), 6.89 (dd, $^3J_{H,H}$ = 9.9 Hz, $^4J_{H,H}$ = 1.8 Hz, 1H, H4), 7.04 (br d, $^3J_{H,H}$ = 7.6 Hz, 1H, H8 or 12), 7.42 (br d, $^3J_{H,H}$ = 7.6 Hz, 1H, H8 or 12), 7.52 (dd, $^3J_{H,H}$ = 7.6 Hz, $^4J_{H,H}$ = 1.3 Hz, 2H, H9 + H11), 7.55 (dd, $^3J_{H,H}$ = 9.9 Hz, $^5J_{H,H}$ = 0.7 Hz, 1H, H3), 8.94 (br s, 1H, NOH) ppm. ^{13}C NMR (100 MHz, $CDCl_3$): δ = 117.3 (C6), 117.7 (C3), 123.5 (C8 or 12), 125.0 (C8 or 12), 130.1 (C9 or 11), 130.4 (C9 or 11), 130.9 (C4), 134.4 (C10), 143.1 (C5), 147.9 (C7), 154.8 (C2), 163.0 (C1), 176.3 (CO), 192.9 (CO), 194.2 (CO) ppm. IR (KBr, cm^{-1}): $\tilde{\nu}$ = 3101 (w), 3084 (w), 2037 ν(CO) (vs), 1953 ν(CO) (vs), 1940 ν(CO) (vs), 1930 ν(CO) (vs), 1604 ν(C=N) (m), 1544 ν(C=N) (w), 1483 (m), 1423 (m), 1264 (s), 1193 (m), 1153 (w), 1056 ν(N—O) (s), 1047 ν(N—O) (m), 1014 (m), 932 (m), 824 (w), 798 (w), 585 (w) 516 (m), 443 (w). **IR** (THF, cm^{-1}): $\tilde{\nu}$ = 2030 ν(CO) (vs), 1954 ν(CO) (m), 1921 ν(CO) (m). IR (CH_2Cl_2, cm^{-1}): $\tilde{\nu}$ = 2034 ν(CO) (vs), 1955 ν(CO) (m), 1928 ν(CO) (m). UV/Vis (CH_2Cl_2): λ_{max} (ε) = 358 (6200), 475 (5400), 549 nm (11000 M^{-1} cm^{-1}). MS (FAB^+): *m/z* (%) = 617.8 (86) [M^+], 589.8 (47) [M^+–CO], 537.0 (100) [M^+–Br], 533.9 (81) [M^+–3CO], 453.0 (73) [M^+–3CO–Br]. $C_{15}H_8BrCl_2N_2O_4Re$ (617.25 g mol^{-1}): calcd. C 29.19, H 1.31, N 4.54; found C 29.03, H 1.29, N 4.39.

*3.3.6. Bromido-tricarbonyl-{4-chloro-o-quinone-(N-p-tolyl)-oximine-N,N′}rhenium(I) (**7b**)*

Reagents: 129 mg (0.318 mmol) **5**, 78 mg (0.318 mmol) **3b**, reaction time: 23 h. Yield: 167 mg (0.280 mmol, 88%), dark green powder. Dark red crystals were obtained by slow isothermic diffusion of *n*-pentane into a solution of **7b** in dichloromethane. – ^{1}H NMR (270 MHz, $CDCl_3$): δ = 2.45 (s, 3H, CH_3), 6.79 (dd, $^4J_{H,H}$ = 1.8 Hz, $^5J_{H,H}$ = 0.7 Hz, 1H, H6), 6.87 (dd, $^3J_{H,H}$ = 9.9 Hz, $^4J_{H,H}$ = 1.8 Hz, 1H, H4), 6.93–7.03 (m, 1H, H8 or 12), 7.29–7.35 (m, 3H, H9 + H11 + H8 or 12), 7.51 (dd, $^3J_{H,H}$ = 9.9 Hz, $^5J_{H,H}$ = 0.7 Hz, 1H, H3), 8.31 (br s, 1H, NOH) ppm. ^{13}C NMR (100 MHz, $CDCl_3$): δ = 21.3 (CH_3), 117.5 (C3), 117.7 (C6), 121.9 (C8 or 12), 123.4 (C8 or 12), 130.3 (C9 or 11), 130.6 (C9 or 11), 131.1 (C4), 138.8 (C10), 142.2 (C5), 147.2 (C7), 154.8 (C2), 162.5 (C1), 176.6 (CO), 193.1 (CO), 194.5 (CO) ppm. IR (KBr, cm^{-1}): $\tilde{\nu}$ = 3097 (w), 3089 (w), 3024 (w), 2919 (w), 2034 ν(CO) (vs), 1957 ν(CO) (vs), 1951 ν(CO) (vs), 1939 ν(CO) (vs), 1925 ν(CO) (vs), 1604 ν(C=N) (m), 1544 ν(C=N) (w), 1502 (m), 1454 (w), 1423 (m), 1267 (s), 1240 (m), 1193 (m), 1153 (m), 1055 ν(N–O) (s), 932 (w), 795 (m), 623 (w) 586 (w), 514 (w). IR (THF, cm^{-1}): $\tilde{\nu}$ = 2030 ν(CO) (vs), 1952 ν(CO) (m), 1919 ν(CO) (m). IR

(CH_2Cl_2, cm^{-1}): $\tilde{\nu}$ = 2032 ν(CO) (vs), 1953 ν(CO) (s), 1926 ν(CO) (s). UV/Vis (CH_2Cl_2): λ_{max} (ε) = 357 (5400), 481 (5500), 544 nm (9900 $M^{-1}\,cm^{-1}$). MS (FAB^+): *m/z* (%) = 596.0 (83) [M^+], 568.0 (44) [M^+–CO], 517.2 (100) [M^+–Br], 512.1.0 (84) [M^+–3CO], 433.1 (75) [M^+–Br–3CO]. $C_{16}H_{11}BrClN_2O_4Re$ (596.83 g mol^{-1}): calcd. C 32.20, H 1.86, N 4.69; found C 32.53, H 1.89, N 4.57.

3.3.7. Bromido-tricarbonyl-{4-chloro-o-quinone-(N-2-chlorophenyl)-oximine-N,N′}rhenium(I) (**7c**)

Reagents: 118 mg (0.291 mmol) **5**, 78 mg (0.291 mmol) **3c**, reaction time: 22 h. Yield: 154 mg (0.250 mmol, 86%), dark purple powder. Black crystals were obtained by slow isothermic diffusion of *n*-pentane into a solution of **7c** in dichloromethane. – ^{1}H NMR (270 MHz, $CDCl_3$): δ = 6.54 (dd, $^4J_{H,H}$ = 1.8 Hz, $^5J_{H,H}$ = 0.7 Hz, 1H, H6), 6.89 (dd, $^3J_{H,H}$ = 9.9 Hz, $^4J_{H,H}$ = 1.8 Hz, 1H, H4), 7.37 (ddd, $^3J_{H,H}$ = 7.9 Hz, $^3J_{H,H}$ = 7.5 Hz, $^4J_{H,H}$ = 1.8 Hz, 1H, H10), 7.46 (ddd, $^3J_{H,H}$ = 7.8 Hz, $^3J_{H,H}$ = 7.5 Hz, $^4J_{H,H}$ = 1.5 Hz, 1H, H11), 7.58 (dd, $^3J_{H,H}$ = 9.9 Hz, $^5J_{H,H}$ = 0.7 Hz, 1H, H3), 7.58 (ddd, $^3J_{H,H}$ = 7.9 Hz, $^4J_{H,H}$ = 1.5 Hz, $^5J_{H,H}$ = 0.4 Hz, 1H, H9), 7.64 (ddd, $^3J_{H,H}$ = 7.8 Hz, $^4J_{H,H}$ = 1.8 Hz, $^5J_{H,H}$ = 0.4 Hz, 1H, H12), 9.50 (br s, 1H, NOH) ppm. ^{13}C NMR (100 MHz, $CDCl_3$): δ = 117.3 (C6), 117.6 (C3), 125.7 (C12), 126.1 (C8), 128.4 (C11), 129.5 (C10), 130.6 (C4), 130.6 (C9), 143.2 (C5), 146.2 (C7), 154.3 (C2), 163.8 (C1), 176.3 (CO), 193.0 (CO), 194.2 (CO) ppm. IR (KBr, cm^{-1}): $\tilde{\nu}$ = 3097 (w), 3086 (w), 2025 ν(CO) (vs), 1956 ν(CO) (vs), 1947 ν(CO) (vs), 1934 ν(CO) (vs), 1926 ν(CO) (vs), 1602 ν(C=N) (m), 1544 ν(C=N) (m), 1468 (m), 1453 (w), 1425 (m), 1391 (w), 1278 (s), 1198 (w), 1149 (w), 1060 ν(N–O) (s), 1047 ν(N–O) (m), 948 (w), 935 (w), 806 (m), 625 (w), 586 (w), 518 (w), 452 (w). IR (THF, cm^{-1}): $\tilde{\nu}$ = 2031 ν(CO) (vs), 1954 ν(CO) (m), 1926 ν(CO) (m). IR (CH_2Cl_2, cm^{-1}): $\tilde{\nu}$ = 2034 ν(CO) (vs), 1955 ν(CO) (m), 1935 ν(CO) (m). UV/Vis (CH_2Cl_2): λ_{max} (ε) = 362 (6400), 441 (3800), 474 (4400), 557 nm (11200 $M^{-1}\,cm^{-1}$). MS (FAB^+): *m/z* (%) = 617.9 (92) [M^+], 589.8 (33) [M^+–CO], 537.0 (100) [M^+–Br], 534.0 (21) [M^+–3CO], 509.0 (13) [M^+–Br–CO], 496.0 (37) [M^+–3CO–H–Cl], 481.0 (12) [M^+–Br–2CO], 453.0 (58) [M^+–Br–3CO], 452.0 (54) [M^+–Br–3CO–H], 417.1 (16) [M^+–Br–3CO–H–Cl]. $C_{15}H_8BrCl_2N_2O_4Re$ (617.25 g mol^{-1}): calcd. C 29.19, H 1.31, N 4.54; found C 29.26, H 1.45, N 4.55.

3.3.8. Bromido-tricarbonyl-{4-chloro-o-quinone-(N-phenyl)-oximine-N,N′}rhenium(I) (**7d**)

Reagents: 141 mg (0.347 mmol) **5**, 81 mg (0.347 mmol) **3d**, reaction time: 20 h. Yield: 178 mg (0.305 mmol, 88%), dark purple powder. Black crystals were obtained by slow isothermic diffusion of *n*-pentane into a solution of **7d** in dichloromethane. – ^{1}H NMR (270 MHz, $CDCl_3$): δ = 6.75 (dd, $^4J_{H,H}$ = 1.8 Hz, $^5J_{H,H}$ = 0.7 Hz, 1H, H6), 6.88 (dd, $^3J_{H,H}$ = 9.9 Hz, $^4J_{H,H}$ = 1.8 Hz, 1H, H4), 7.08 (br d, $^3J_{H,H}$ = 7.2 Hz, 1H, H8 or 12), 7.42 (dddd, $^3J_{H,H}$ = 7.3 Hz, $^3J_{H,H}$ = 7.3 Hz, $^4J_{H,H}$ = 1.4 Hz, $^4J_{H,H}$ = 1.4 Hz, 1H, H10), 7.43–7.48 (m, 1H, H8 or 12), 7.50–7.58 (m, 2H, H9 + H11), 7.53 (dd, $^3J_{H,H}$ = 9.9 Hz, $^5J_{H,H}$ = 0.7 Hz, 1H, H3), 8.53 (br s, 1H, NOH) ppm. ^{13}C NMR (100 MHz, $CDCl_3$): δ = 117.6 (C3), 117.6 (C6), 122.0 (C8 or 12), 123.4 (C8 or 12), 128.6 (C10), 129.8 (C9 or 11), 130.1 (C9 or 11), 131.0 (C4), 142.5 (C5), 149.6 (C7), 154.8 (C2), 162.7 (C1), 176.4 (CO), 193.0 (CO), 194.4 (CO) ppm. IR (KBr, cm^{-1}): $\tilde{\nu}$ = 3106 (w), 3083 (w), 2038 ν(CO) (vs), 1959 ν(CO) (vs), 1925 ν(CO) (vs), 1908 ν(CO) (vs), 1597 ν(C=N) (m), 1545 ν(C=N) (m), 1451 (m), 1418 (w), 1392 (m), 1285 (s), 1184 (w), 1151 (w), 1051 ν(N–O) (s), 1042 ν(N–O) (m), 938 (w), 803 (m), 763 (w), 703 (m), 623 (w), 579 (w) 540 (w). IR (THF, cm^{-1}): $\tilde{\nu}$ = 2030 ν(CO) (vs), 1953 ν(CO) (m), 1920 ν(CO) (m). IR (CH_2Cl_2, cm^{-1}): $\tilde{\nu}$ = 2033 ν(CO) (vs), 1954 ν(CO) (m), 1927 ν(CO) (m). UV/Vis (CH_2Cl_2): λ_{max} (ε) = 358 (5600), 473 (4700), 546 nm (9800 $M^{-1}\,cm^{-1}$). MS (FAB^+): *m/z* (%) = 582.0 (87) [M^+], 554.0 (46) [M^+–CO], 503.1 (100) [M^+–Br], 498.1 (74) [M^+–3CO], 419.2 (67) [M^+–Br–3CO]. $C_{15}H_9BrClN_2O_4Re$ (582.81 g mol^{-1}): calcd. C 30.91, H 1.56, N 4.81; found C 31.24, H 1.64, N 4.74.

3.4. Cell culture conditions and drug treatment

Tested oximine rhenium(I) complexes and ligands were diluted in DMSO and stored at −20 °C. Working solutions were prepared in RPMI 1640 medium immediately before use. The human K562 cell line was a gift of Prof. Jean Claude D'Halluin (INSERM 125, Lille, France). This Bcr–Abl-positive cell line was maintained as described previously [79]. For experiments, K562 cells were seeded at the density 3.5×10^4 mL^{-1}, 22 h later the tested rhenium(I) complexes or ligands at indicated concentrations were added to cells cultured in suspension. A375, a human melanoma adherent cell line with high metastatic potential, derived from a 54 year old female with malignant melanoma (a gift of Prof. Piotr Laidler, Jagiellonian University, Poland) was maintained in RPMI 1640 medium supplemented with 10% FBS and antibiotics. For drug exposure experiments, culture medium was substituted with fresh medium containing 0.5% FBS and tested compounds at indicated concentrations. Equivalent final concentration of DMSO was used in the control cultures.

3.5. Proliferation and viability of cancer cells

3.5.1. Leukemia cell viability and proliferation assay

Cell proliferation and viability were determined by using Trypan blue dye exclusion assay (Sigma-Aldrich, St. Louis, MO, USA). K562 cells were seeded at the density 4×10^4 mL^{-1}, 22 h later the oximine rhenium(I) complexes or ligands were added at indicated concentrations. Non-treated cells were cultivated as control. Proliferation rate or cell viability was evaluated as described previously [79]. Briefly, treatment with drugs was carried out up to 3 days and aliquots were removed daily for determination of dead and viable cell number using Trypan blue dye exclusion test. In proliferation assay, only viable cells were counted that did not take up Trypan blue. Comparison was made relative to values obtained for the untreated control and expressed as percentage of the control. In viability assay, the number of viable cells not taking up Trypan blue is expressed as percentage of the total cell number (viable and dead) in each experimental condition. The medium was not changed during the induction period. Each experiment was conducted in triplicate and repeated three times.

3.5.2. Melanoma cell proliferation assay

Cell proliferation was measured by a colorimetric MTT (3-(4,5-Dimethylthiazol-2-yl)-2,5-diphenyltetrazolium bromide) assay. Briefly, cells were seeded in 24-well plates and allowed to adhere for 6 h in medium containing 10% fetal bovine serum (FBS). Next, they were treated for 2 days with tested compounds at indicated concentrations in the culture medium containing 0.5% FBS. MTT reagent (thiazolyl blue tetrazolium bromide; Sigma-Aldrich; 0.84 mg mL^{-1} in PBS) was added and left in the cultures for 3 h at 37 °C prior to addition of 800 µL solubilization reagent (DMSO in optical grade). The reduction of a tetrazolium component into DMSO-soluble formazan product was monitored at a wavelength of 540 nm using a spectrophotometer. The mean of the absolute absorbance values given by drug-treated cells was divided by the mean of the absolute absorbance of DMSO-treated control sample and expressed as relative number of viable adherent cells. Data show the mean of at least three independent experiments ± SD. IC_{50} was calculated. For time course, the number of viable, adherent melanoma cells was estimated each day by MTT assay after incubation with tested compounds at the concentration of 1.4 µM.

3.5.3. Flow cytometric analysis of melanoma cell viability

The cytotoxicity of tested compounds on cultured melanoma cells was detected by propidium iodide (PI; Sigma) staining and FACS analysis. Cells were treated with tested drugs at indicated

Table 5
Crystal data and details of structural refinement on **3b**, **3d** and **6a**–**7d**.

	3b	**3d**	**6a**	**6b**	**6c**	**6d**	**7a**	**7b**	**7c**	**7d**
Formula	$C_{13}H_{11}ClN_2O$	$C_{12}H_9ClN_2O$	$C_{15}H_8Cl_3N_2O_4Re$	$C_{16}H_{11}Cl_2N_2O_4Re$	$C_{16}H_{10}Cl_5N_2O_4Re$	$C_{15}H_9Cl_2N_2O_4Re$	$C_{15}H_8BrCl_2N_2O_4Re$	$C_{21}H_{23}BrClN_2O_4Re$	$C_{16}H_{10}BrCl_4N_2O_4Re$	$C_{16}H_{11}BrCl_3N_2O_4Re$
FW [g mol^{-1}]	246.692	232.665	572.800	552.382	657.732	538.355	617.251	668.982	702.183	667.739
Temperature [K]	200(2)	200(2)	200(2)	200(2)	200(2)	200(2)	200(2)	200(2)	200(2)	200(2)
Wavelength [Å]	0.71073	0.71073	0.71073	0.71073	0.71073	0.71073	0.71073	0.71073	0.71073	0.71073
Crystal system	Monoclinic	Monoclinic	Triclinic	Triclinic	Triclinic	Triclinic	Triclinic	Triclinic	Triclinic	Monoclinic
Space group	*P*21/*c*	*P*21/*c*	*P*-1	*P*-1	*P*-1	*P*-1	*P*-1	*P*-1	*P*-1	*C*2/*c*
a [Å]	9.957(2)	10.599(2)	8.862(2)	8.754(2)	9.273(2)	9.027(2)	6.769(2)	6.777(2)	9.344(2)	25.708(5)
b [Å]	15.364(3)	6.658(2)	10.524(2)	10.732(2)	10.129(2)	9.796(2)	11.821(2)	11.949(2)	10.198(2)	10.095(2)
c [Å]	8.390(2)	15.413(3)	11.074(2)	11.525(2)	11.110(2)	10.499(2)	12.065(2)	15.573(3)	11.318(2)	17.501(3)
α (°)	90	90	71.76(3)	116.22(3)	86.19(3)	109.38(3)	93.42(3)	69.53(3)	86.08(3)	90
β (°)	112.38(3)	99.59(3)	66.85(3)	101.44(3)	85.36(3)	101.12(3)	105.14(3)	88.26(3)	85.79(3)	102.45(3)
γ (°)	90	90	80.71(3)	101.02(3)	79.82(3)	99.30(3)	102.05(3)	77.92(3)	80.49(3)	90
V [Å^3]	1186.9(5)	1072.4(4)	901.0(4)	902.9(5)	1022.2(4)	833.5(4)	904.7(3)	1153.9(5)	1059.1(4)	4435.1(15)
Z	4	4	2	2	2	2	2	2	2	8
$\rho_{calc.}$ [g cm^{-3}]	1.3806	1.4411	2.1114	2.0318	2.1370	2.1451	2.2659	1.9254	2.2019	2.0001
μ [mm^{-1}]	0.305	0.333	7.210	7.048	6.623	7.631	9.242	7.141	8.152	7.665
F(000)	512	480	540	524	624	508	576	644	660	2512
Crystal size [mm]	0.16×0.13×0.02	0.33×0.18×0.16	0.30×0.17×0.12	0.11×0.10×0.09	0.23×0.22×0.14	0.17×0.08×0.02	0.21×0.12×0.10	0.19×0.16×0.13	0.24×0.18×0.15	0.16×0.08×0.03
θ range [°]	3.45–25.37	3.90–26.34	3.88–26.35	3.28–27.52	3.17–27.56	3.70–25.50	3.20–26.41	3.73–26.35	3.70–26.33	3.16–27.00
Index ranges	$-11\le h\le 11$ $-18\le k\le 17$ $-10\le l\le 10$	$-13\le h\le 10$ $-8\le k\le 6$ $-19\le l\le 19$	$-11\le h\le 11$ $-13\le k\le 13$ $-13\le l\le 13$	$-11\le h\le 11$ $-13\le k\le 13$ $-14\le l\le 14$	$-12\le h\le 12$ $-13\le k\le 12$ $-14\le l\le 14$	$-10\le h\le 10$ $-10\le k\le 11$ $-12\le l\le 12$	$-8\le h\le 8$ $-14\le k\le 14$ $-15\le l\le 15$	$-8\le h\le 8$ $-14\le k\le 14$ $-19\le l\le 19$	$-10\le h\le 11$ $-12\le k\le 12$ $-13\le l\le 14$	$-32\le h\le 32$ $-12\le k\le 12$ $-21\le l\le 22$
Reflns collected	7202	4750	10164	19819	22333	5763	17978	9553	10588	40519
Independent reflns	2151	2166	3644	4122	4681	3068	3700	4655	4281	4832
R_{int}	0.0420	0.0284	0.0304	0.0389	0.0610	0.0587	0.0328	0.0282	0.0249	0.0474
Completeness to θ [%]	99.0	99.0	99.3	99.4	99.2	99.0	99.5	98.9	99.2	99.6
Refinement method	Full-matrix least-squares on F^2	Full-matrix least-squares on F^2	Full-matrix least-squares on F^2	Full-matrix least-squares on F^2	Full-matrix least-squares on F^2	Full-matrix least-squares on F^2	Full-matrix least-squares on F^2	Full-matrix least-squares on F^2	Full-matrix least-squares on F^2	Full-matrix least-squares on F^2
Data/restraints/ parameters	2151/0/159	2166/0/149	3644/0/227	4122/0/228	4681/2*/239	3068/0/219	3700/0/227	4655/0/226	4281/2*/239	4832/10*/264
Goodness-of-fit on F^2	1.039	0.876	0.964	1.036	1.046	0.909	1.153	1.023	1.056	1.060
Final *R* indices [$I>2\sigma(I)$]	$R_1=0.0374$ $wR_2=0.0872$	$R_1=0.0355$ $wR_2=0.0766$	$R_1=0.0207$ $wR_2=0.0389$	$R_1=0.0216$ $wR_2=0.0447$	$R_1=0.0399$ $wR_2=0.1021$	$R_1=0.0442$ $wR_2=0.0818$	$R_1=0.0213$ $wR_2=0.0478$	$R_1=0.0239$ $wR_2=0.0535$	$R_1=0.0359$ $wR_2=0.1001$	$R_1=0.0371$ $wR_2=0.0906$
R indices (all data)	$R_1=0.0580$ $wR_2=0.0979$	$R_1=0.0631$ $wR_2=0.0813$	$R_1=0.0270$ $wR_2=0.0395$	$R_1=0.0257$ $wR_2=0.0458$	$R_1=0.0471$ $wR_2=0.1065$	$R_1=0.0707$ $wR_2=0.0876$	$R_1=0.0236$ $wR_2=0.0487$	$R_1=0.0331$ $wR_2=0.0567$	$R_1=0.0459$ $wR_2=0.1033$	$R_1=0.0505$ $wR_2=0.0993$
Largest diff. peak/ hole [e Å^{-3}]	0.208 and −0.218	0.176 and −0.205	1.291 and −0.710	0.805 and −0.897	2.051 and −2.413	2.348 and −1.723	0.586 and −0.851	1.328 and −0.740	2.548 and −1.803	1.672 and −1.518
CCDC number	730545	730546	730547	730548	730549	730550	730551	730552	730553	730554

*Restraints only used for refinement of solvent molecules.

concentrations for 2 days. After treatment, both attached (harvested by trypsinization) and floating cells were collected, centrifuged at 400×*g* for 5 min and stained with PI (8 μg mL^{-1}) for 10 min at room temperature in the dark. PI-positive cells were identified on a FACSCalibur (Becton Dickinson). 10,000 events were analyzed for each sample and results were processed by using CellQuest software (Becton Dickinson).

3.6. Fluorescence microscopy

3.6.1. Acridine orange/ethidium bromide staining

Cell death was studied morphologically using fluorescent dyes: acridine orange (AO) and ethidium bromide (EB). Briefly, the melanoma cells were cultured for 2 days and leukemia cells for 3 days with or without tested agents at indicated concentrations. Cells (1×10^5) were collected by centrifugation and resuspended in 20 μL of staining solution mixture of 100 μg mL^{-1} of EB and 100 μg mL^{-1} of AO (1:1) (Sigma Chemical Co.). Then, they were examined by ultraviolet fluorescence microscopy (Olympus BX 41). In each experiment, more than 300 cells were analyzed and then percentages of early/late apoptotic or necrotic cells were calculated. The cells with bright green chromatin with organized structure were counted as viable. The cells with green, condensed and fragmented chromatin were counted as early apoptotic cells. In late apoptotic cells, chromatin was condensed or fragmented and stained orange. Necrotic cells had bright orange chromatin with organized structure.

3.6.2. DAPI staining

Apoptosis was also evaluated by DAPI (4′,6′-diamidino-2-phenylindole) staining. K562 cells were cultured for 3 days with or without tested compounds at indicated concentrations. 5×10^5 cells were collected by centrifugation, washed with PBS and fixed with ice-cold 70% ethanol overnight at −20 °C. After washings in PBS, cells were incubated for 10 min with 20 μM DAPI (0.5 μg mL^{-1}, Molecular Probes, Eugene, Oregon, USA) at room temperature in the darkness. Finally, the cells were examined by ultraviolet fluorescence microscopy (Olympus BX 41). Apoptotic cells were identified qualitatively as cells with condensed chromatin and fragmented nuclei.

3.7. Statistical analysis

Data represent the mean ± SD from at least three separate experiments. The significance of an apparent difference in mean values for any tested parameter was validated by a Student's paired *t* test. The difference was considered significant if $P<0.05$. IC_{50} values were calculated by concentration–response curve fitting using a Microsoft Excel-based analytic method.

3.8. X-ray structure determinations

Single crystal X-ray diffraction data were collected on a Nonius Kappa CCD and a Oxford Diffraction Xcalibur S, both using graphite-monochromated Mo-*Kα* radiation (λ = 0.71073 Å). Semi-empirical absorption correction using equivalent reflections were applied if not stated otherwise. Structures were solved by Direct Methods with the SHELXS program and refined by full-matrix least-squares using SHELXL-97 [80,81]. All non-hydrogen atoms except solvent molecules in **6c** and **7c** were refined with anisotropic displacement parameters. The PLATON [82]/SQUEEZE [83] software was applied to subtract the contribution of disordered solvent from diffraction data of **7b** (pentane) as no reasonable modelling was possible during refinement. It has been treated as diffuse contribution to the overall scattering without specific atom positions. The exclusion of the solvent seems to have no effect on the structure since no hydrogen bonding was observed to this solvent molecule. SQUEEZE details are appended to the deposited final refinement CIFs. The CCDC numbers in Table 5 contain the supplementary crystallographic data for this paper. These data can be obtained free of charge from The Cambridge Crystallographic Data Centre via http://www.ccdc.cam.ac.uk/data_request/cif.

4. Conclusions

The present paper has reported the synthesis of the first *o*-quinoid oximine complexes. Two series of halogenido Re(I) compounds (X=Cl, Br) have been synthesized and subjected to full spectroscopic characterisation to ensure a systematic approach to this new configuration. Two ligands known from literature and two new ligands have been employed for this study. Structures from all novel complexes (**6a–7d**) and from two of the ligands (**3b and 3d**) have been confirmed by single crystal X-ray crystallography, so there is no doubt about the reported oximine character and the proton shift. Biological studies have revealed that the newly synthesized oximine rhenium(I) complexes could induce apoptotic cell death in leukemia and melanoma cells, thus reducing proliferation of drug-treated cancer cells. Chlorido complexes (**6a** and **6c**) were more efficient than bromido compounds (**7d** and **7b**) in stimulating apoptosis. None of the tested ligands (**3a–d**) showed any significant anticancer activity. As systematic investigations in this ligand system just started, work on a larger variety of functional groups and transition metals is in progress at the moment. First experiments with different metal centers indicate that the proton shift cannot be anticipated in general.

Acknowledgments

Financial support by the Center for Integrated Protein Science Munich (CIPS, LMU Excellent) is gratefully acknowledged. We are grateful to Dr. Marta Stasiak for her help in FACS and Mrs. Grazyna Kus for technical work. This research was supported by Grant 503-1099-2 from the Medical University of Lodz.

References

[1] A. Baeyer, C. Caro, Ber. Dtsch. Chem. Ges. 7 (1874) 809–811.
[2] A. Baeyer, Ber. Dtsch. Chem. Ges. 7 (1874) 1638–1640.
[3] R.H. Pickard, J. Kenyon, J. Chem. Soc., Trans. 91 (1907) 896–905.
[4] B.G. Gowenlock, G.B. Richter-Addo, Chem. Rev. 104 (2004) 3315–3340.
[5] B.G. Gowenlock, G.B. Richter-Addo, Chem. Soc. Rev. 34 (2005) 797–809.
[6] M. Cameron, B.G. Gowenlock, G. Vasapollo, Chem. Soc. Rev. 19 (1990) 355–379.
[7] H. Yamamoto, N. Momiyama, Chem. Commun. (2005) 3514–3525.
[8] P. Ehrlich, F. Sachs, Ber. Dtsch. Chem. Ges. 32 (1899) 2341–2346.
[9] W. Adam, O. Krebs, Chem. Rev. 103 (2003) 4131–4146.
[10] H. Waldmann, Synthesis 1994 (1994) 535–551.
[11] J. Streith, A. Defoin, Synthesis 1994 (1994) 1107–1117.
[12] P.F. Vogt, M.J. Miller, Tetrahedron 54 (1998) 1317–1348.
[13] D. Keilin, E.F. Hartree, Nature 151 (1940) 390–391.
[14] Q.H. Gibson, Biochem. J. 77 (1960) 519–526.
[15] M. Murayama, J. Biol. Chem. 235 (1960) 1024–1028.
[16] J.B. Schenkman, B.J. Wilson, D.L. Cinti, Biochem. Pharmacol. 21 (1972) 2373–2383.
[17] M.R. Franklin, Mol. Pharmacol. 10 (1974) 975–985.
[18] D. Mansuy, P. Beaune, J.C. Chottard, J.F. Bartoli, P. Gans, Biochem. Pharmacol. 25 (1976) 609–612.
[19] D. Mansuy, P. Battioni, J.C. Chottard, M. Lange, J. Am. Chem. Soc. 99 (1977) 6441–6443.
[20] D. Mansuy, P. Beaune, T. Cresteil, C. Bacot, J.-C. Chottard, P. Gans, Eur. J. Biochem. 86 (1978) 573–579.
[21] J. Lee, L. Chen, A.H. West, G.B. Richter-Addo, Chem. Rev. 102 (2002) 1019–1066.
[22] Z. Wrobel, A. Kwast, Synlett (2007) 1525–1528.
[23] R. Wilberger, C. Krinninger, H. Piotrowski, P. Mayer, I.-P. Lorenz, Eur. J. Inorg. Chem. (2004) 2488–2492.
[24] C. Krinninger, C. Högg, H. Nöth, J.C.G. Ruiz, P. Mayer, O. Burkacky, A. Zumbusch, I.-P. Lorenz, Chem. Eur. J. 11 (2005) 7228–7236.
[25] C. Krinninger, S. Wirth, P. Klüfers, P. Mayer, I.P. Lorenz, Eur. J. Inorg. Chem. (2006) 1060–1066.
[26] C. Krinninger, S. Wirth, J.C.G. Ruiz, P. Klüfers, H. Nöth, I.-P. Lorenz, Eur. J. Inorg. Chem. (2005) 4094–4098.
[27] M. Okubo, Y. Inatomi, N. Taniguchi, K. Imamura, Bull. Chem. Soc. Jpn. 61 (1988) 3581–3585.
[28] H. Pesari, D. Grasso, Biotechnol. Bioeng. 41 (1993) 79–87.
[29] F.D. Denonne, P. Seiler, F. Diederich, Helv. Chim. Acta 86 (2003) 3096–3117.
[30] E. Fasani, S. Pietra, A. Albini, Heterocycles 33 (1992) 573–584.
[31] E. Fasani, M. Mella, A. Albini, J. Chem. Soc., Perkin Trans. 1 (1992) 2689–2692.

[32] S.P. Titova, A.K. Arinich, M.V. Gorelik, J. Org, Chem. USSR 5 (1986) 1407–1408.
[33] H. Böhme, J. Nehne, Arch. Pharm. 313 (1980) 454–461.
[34] D. Jin, D.G. Mendenhall, Tetrahedron Lett. 37 (1996) 4881–4882.
[35] I.L. Eremenko, S.E. Nefedov, A.A. Sidorov, M.O. Ponina, P.V. Danilov, T.A. Stromnova, I.P. Stolarov, S.B. Katser, S.T. Orlova, M.N. Vargaftik, I.I. Moiseev, Y.A. Ustynyuk, J. Organomet. Chem. 551 (1998) 171–194.
[36] S.T. Orlova, D.N. Kazyul'kin, L.K. Shubochkin, D.I. Shishkin, T.A. Stromnova, Russ. Chem. Bull. 50 (2001) 1689–1692.
[37] T.A. Stromnova, S.T. Orlova, Russ. Chem. Bull. 51 (2002) 2286–2289.
[38] S.T. Orlova, T.A. Stromnova, D.N. Kazyul'kin, L.I. Boganova, D.I. Kochubey, B.N. Novgorodov, Russ. Chem. Bull. 53 (2004) 819–824.
[39] H. Schöllhorn, U. Thewalt, B. Lippert, J. Am. Chem. Soc. 111 (1989) 7213–7221.
[40] B. Lippert, H. Schöllhorn, U. Thewalt, Inorg. Chim. Acta 198–200 (1992) 723–732.
[41] M.-a. Haga, M.M. Ali, S. Koseki, K. Fujimoto, A. Yoshimura, K. Nozaki, T. Ohno, K. Nakajima, D.J. Stufkens, Inorg. Chem. 35 (1996) 3335–3347.
[42] M.R. Arkin, E.D.A. Stemp, R.E. Holmlin, J.K. Barton, A. Hormann, E.J.C. Olson, P.F. Barbara, Science 273 (1996) 475–480.
[43] P.K.-L. Fu, P.M. Bradley, C. Turro, Inorg. Chem. 42 (2003) 878–884.
[44] J. Rall, A.F. Stange, K. Hübler, W. Kaim, Angew. Chem. Int. Ed. 37 (1998) 2681–2682.
[45] I.G. Fomina, A.A. Sidorov, G.G. Aleksandrov, S.E. Nefedov, I.L. Eremenko, I.I. Moiseev, J. Organomet. Chem. 636 (2001) 157–163.
[46] S. Frantz, J. Rall, I. Hartenbach, T. Schleid, S. Záliscaron, W. Kaim, Chem. Eur. J. 10 (2004) 149–154.
[47] S.I. Gorelsky, E.S. Dodsworth, A.B.P. Lever, A.A. Vlcek, Coord. Chem. Rev. 174 (1998) 469–494.
[48] A.B.P. Lever, S.I. Gorelsky, Coord. Chem. Rev. 208 (2000) 153–167.
[49] L.D. Brown, D.W. Kalina, M.S. McClure, S. Schultz, S.L. Ruby, J.A. Ibers, C.R. Kannewurf, T.J. Marks, J. Am. Chem. Soc. 101 (1979) 2937–2947.
[50] M. Mégnamisi-Bélomeé, J. Solid State Chem. 27 (1979) 389–396.
[51] I. Shirotani, T. Kudo, N. Sato, H. Yamochi, G. Saito, J. Mater. Chem. 5 (1995) 1357–1362.
[52] K.-i. Sakai, T. Hasegawa, M. Ichikawa, Y. Taniguchi, Chem. Lett. 35 (2006) 302–303.
[53] M. Cameron, B.G. Gowenlock, R.V. Parish, G. Vasapollo, J. Organomet. Chem. 465 (1994) 161–166.
[54] L. Lunazzi, D. Macciantelli, G. Placucci, Tetrahedron Lett. 21 (1980) 975–976.
[55] A.S.F. Boyd, G. Browne, B.G. Gowenlock, P. McKenna, J. Organomet. Chem. 345 (1988) 217–220.
[56] M. Cameron, B.G. Gowenlock, G. Vasapollo, J. Organomet. Chem. 378 (1989) 493–496.
[57] L.J. Farrugia, J. Appl. Cryst., 1997.
[58] C.A. Hunter, J.K.M. Sanders, J. Am. Chem. Soc. 112 (1990) 5525–5534.
[59] C. Janiak, Dalton Trans. (2000) 3885–3896.
[60] E. Canpolat, M. Kaya, Russ. J. Coord. Chem. 31 (2005) 415–419.
[61] M. Kaya, C. Yenikaya, A. Colak, F. Colak, Russ. J. Gen. Chem. 78 (2008) 1808–1815.
[62] V. Alexander, Inorg. Chim. Acta 204 (1993) 109–124.
[63] V.K. Sharma, S. Srivastava, J. Coord. Chem. 61 (2008) 178–191.
[64] C. Várhelyi Jr, G. Pokol, Á. Gömöry, A. Gănescu, P. Sohár, G. Liptay, C. Várhelyi, J. Therm. Anal. Calorim. 83 (2006) 701–707.
[65] H. Hartmann, T. Scheiring, J. Fiedler, W. Kaim, J. Organomet. Chem. 604 (2000) 267–272.
[66] N.A. Illán-Cabeza, A.R. García-García, M.N. Moreno-Carretero, J.M. Martínez-Martos, M.J. Ramírez-Expósito, J. Inorg. Biochem. 99 (2005) 1637–1645.
[67] I. Chakraborty, B.K. Panda, J. Gangopadhyay, A. Chakravorty, Inorg. Chem. 44 (2005) 1054–1060.
[68] S. Jurisson, L. Francesconi, K.E. Linder, E. Treher, M.F. Malley, J.Z. Gougoutas, A.D. Nunn, Inorg. Chem. 30 (1991) 1820–1827.
[69] S. Jurisson, M.M. Halihan, J.D. Lydon, C.L. Barnes, D.P. Nowotnik, A.D. Nunn, Inorg. Chem. 37 (1998) 1922–1928.
[70] L. Cuesta, M.A. Huertos, D. Morales, J. Perez, L. Riera, V. Riera, D. Miguel, A. Menendez-Velazquez, S. Garcia-Granda, Inorg. Chem. 46 (2007) 2836–2845.
[71] S. Bhattacharya, P. Gupta, F. Basuli, C.G. Pierpont, Inorg. Chem. 41 (2002) 5810–5816.
[72] M. Czyz, J. Jakubowska, M. Sztiller-Sikorska, Biochem. Pharmacol. 75 (2008) 1761–1773.
[73] A. Jacquel, M. Herrant, L. Legros, N. Belhacene, F. Luciano, G. Pages, P. Hofman, P. Auberger, FASEB J. 17 (2003) 2160–2162.
[74] M.S. Soengas, S.W. Lowe, Oncogene 22 (2003) 3138–3151.
[75] L. Serrone, M. Zeuli, F.M. Sega, F. Cognetti, J. Exp, Clin. Cancer Res. 19 (2000) 21–34.
[76] A.I. Riker, R. Jove, A.I. Daud, Front. Biosci. 11 (2006) 1–14.
[77] S. O'Day, P. Boasberg, Surg. Oncol. Clin. N. Am. 15 (2006) 419–437.
[78] G. Brauer Journal III (1981) Pages.
[79] M. Czyz, A. Szulawska, A.K. Bednarek, M. Düchler, Biochem. Pharmacol. 70 (2005) 1431–1442.
[80] G.M. Sheldrick, University of Göttingen, Göttingen, 1997.
[81] G.M. Sheldrick, Acta Crystallogr., Sect. A 64 (2008) 112–122.
[82] A.L. Spek, J. Appl. Crystallogr. 36 (2003) 7–13.
[83] P. van der Sluis, A.L. Spek, Acta Crystallogr., Sect. A A46 (1990) 187–194.